



Preparation of new half sandwich ruthenium arene complexes with aminophosphines as potential chemotherapeutics

Cristina Aliende ^a, Mercedes Pérez-Manrique ^a, Félix A. Jalón ^b, Blanca R. Manzano ^b, Ana M. Rodríguez ^b, José Vicente Cuevas ^a, Gustavo Espino ^{a,*}, M^a Ángeles Martínez ^c, Anna Massaguer ^d, Marta González-Bártulos ^d, Rafael de Llorens ^d, Virtudes Moreno ^e

^a Departamento de Química, Facultad de Ciencias, Universidad de Burgos, Plaza Misael Bañuelos s/n, 09001, Burgos, Spain

^b Departamento de Química Inorgánica, Orgánica y Bioquímica, Facultad de Químicas, Universidad de Castilla-La Mancha, Avda. Camilo J. Cela 10, 13071, Ciudad Real, Spain

^c Departament de Química, Universitat de Girona, Campus de Montilivi, s/n, 17071, Girona, Spain

^d Departament de Biologia, Facultat de Ciències, Universitat de Girona, Campus de Montilivi, s/n, 17071, Girona, Spain

^e Departament de Química Inorgánica, Universitat de Barcelona, Martí i Franquès 1–11, 08028, Barcelona, Spain

ARTICLE INFO

Article history:

Received 22 March 2012

Received in revised form 31 July 2012

Accepted 31 July 2012

Available online 30 August 2012

Keywords:

Ruthenium(II) arene complexes

Aminophosphines

Anticancer drugs

Cytotoxicity

Metal-based drugs

DNA interaction

ABSTRACT

Aminophosphines 2-(diphenylphosphino)-1-methylimidazole (dpim) and diphenyl-2-pyridylphosphine (PPh₂py) have been used to prepare two series of Ru(II) arene complexes of formulae [(η⁶-p-cymene)Ru(κ²-O,O'-X)(κ¹-P-dpim)]Y (series a: **1a**·Y–**3a**·Y) and [(η⁶-p-cymene)Ru(κ²-O,O'-X)(κ¹-P-PPh₂py)]Y (series b: **1b**·Y–**3b**·Y) (where X = acac, acetylacetonate; bzac, benzoyl acetate; dbzm, dibenzoyl methanoate; Y = BF₄, BPh₄). The structures of **1a**·BF₄, **1a**·BPh₄, **3a**·BF₄, **1b**·BPh₄ and **3b**·BPh₄ were determined by X-ray diffraction. The tetrafluoroborate derivatives are more soluble in organic solvents than their tetraphenylborate counterparts. Five BF₄⁻ derivatives (all except the unstable **1b**·BF₄) were selected to evaluate the cytotoxic behavior *in vitro* against the human cancer cell lines MCF-7 (breast cancer) and CAPAN-1 (pancreatic cancer). **2b**·BF₄ and **3b**·BF₄ exhibited IC₅₀ values similar to those of cisplatin. Electrophoresis and AFM studies showed good correspondence between the biological activity levels of **2b**·BF₄ and **3b**·BF₄ and their ability to modify the DNA structure. Hydrolytic studies indicate that aquation could be involved in the activation mechanism of these complexes and confirm that the hydrolysis rate of **3b**·BF₄ is higher than that of **3a**·BF₄. Thus, the cytotoxic activity trends are explained in terms of the higher reactivity of derivatives from series b, which in turn is rationalized as being the result of the electronic features of dpim and PPh₂py established by cyclic voltammetry measurements.

© 2012 Elsevier Inc. All rights reserved.

1. Introduction

Chemotherapy has become one of the most successful tools in the battle to treat cancer. Indeed, modern societies enjoy a huge battery of different medicines, such as cisplatin and its congeners, to cure certain types of cancer. However, new anticancer drugs are required not only to widen the number of malignant tumors that can be successfully treated, but also to improve the selectivity over tumor tissue types [1]. In particular, the family of organometallic Ru(II) arene complexes is developing very rapidly due to the high activity of some leading complexes against both primary tumors [2–4] and metastasis processes [5,6]. For instance, the [(η⁶-arene)RuCl(en)]PF₆ family, developed by Sadler and co-workers, shows high cytotoxicity to cancer cells, including cisplatin-resistant cells, with DNA as the alleged biological target [4,7,8]. Another significant case is that of [(η⁶-toluene)RuCl₂(pta)] (pta:

1,3,5-triaza-7-phosphatrimethyl[3.3.1]decane) and related complexes developed by the group of Dyson, which show selectivity towards metastatic tumors [9]. It is worth noting that updated perspectives on this issue have been reported in recent reviews [1,9–12].

The attribution of several advantages to Ru as the metal ion has led to particular interest in this family of compounds. These advantages include the following: (i) these compounds show lower general toxicity than Pt drugs, allegedly because they make use of plasma iron-binding proteins such as transferrin to reach the cells [11], (ii) most of the Ru complexes can interact with DNA *in vitro* models but display binding modes and action mechanisms that differ from those of Pt derivatives, and (iii) Ru(II) arene complexes have a versatile stereochemistry that offers multiple possibilities for innovative design and modification, either in the arene or in the three remaining σ-bonded ligands. Similarly, certain opportunities for enhancement have also been emphasized with regard to the performance of the candidates under scrutiny, namely: (i) both selectivity and broadening of the therapeutic action should be improved [12]; (ii) DNA interaction cannot guarantee *in vivo* activity [13]; and (iii) proteins should

* Corresponding author.

E-mail address: gespino@ubu.es (G. Espino).

also be taken into account as pharmacological targets [13]. Thus, in recent years several innovative strategies have been proposed to make progress in this field and these include the following: (a) multifunctional chemotherapy, which aims to identify synergisms between the metallic center and functional ligands [14,15], (b) the use of multinuclear arene ruthenium compounds that focus on the modification of the pharmacological action mechanism [16], (c) photodynamic therapy (PDT), in which nontoxic photosensitive compounds (photosensitizers) are used that are *in situ* activated by specific wavelengths of light [17,18], and (d) catalytic oxidation of glutathione to glutathione disulfide with complexes of formula $[(\eta^6\text{-arene})\text{Ru}(\text{azpy})]^+$ (azpy = N,N-dimethylphenyl or hydroxyphenyl-azopyridine), whose cytotoxic action is based on the accumulation of reactive oxygen species (ROS) in the cancer cells [19].

In particular, our group is attracted by the possibilities of multifunctional chemotherapy. Indeed, we believe that the use of Ru(II) complexes with aminophosphines as functional ligands could provide novel drugs with enhanced cytotoxic properties. Aminophosphines are a class of ligands that have been widely used in catalysis, mainly due to their hemilabile behavior [20]. In this context, we have previously reported the catalytic activity of complexes of general formula $[(\eta^6\text{-p-cym})\text{RuCl}_2(\kappa^1\text{-P-L})]$ (L = 2-(diphenylphosphino)-1-methylimidazole, dpim, **A**; or 2-(diphenylphosphino)pyridine, PPh₂py, **B**) (Scheme 1) [21]. By contrast, aminophosphines have been underutilized in the field of bioorganometallics, with certain well known exceptions. The pioneering work of Dyson et al. has focused on the therapeutic potential of complexes with the hydrophilic phosphine PTA (1,3,5-triaza-7-phosphaadamantane) [1,9,22]. In particular, they have reported that complexes of the type $[(\eta^6\text{-p-cym})\text{Ru}(\kappa^2\text{-O,O'-X})(\text{PTA})\text{Y}]$ (p-cym = p-cymene; X = β -diketonate, Y = BPh₄, BF₄) (see **D** in Scheme 1) are water-soluble and display remarkable cytotoxicity in A2780 human ovarian cancer cells [23]. Previously, Sadler et al. had found that neutral complexes of the class $[(\eta^6\text{-p-cym})\text{Ru}(\kappa^2\text{-O,O'-X})\text{Cl}]$ (X = β -diketonate) are highly cytotoxic (see **C** in Scheme 1) [24]. Thus, inspired by the previous work of Dyson and Sadler, we present here the synthesis and characterization of a new family of Ru(II)-arene complexes with the general formula $[(\eta^6\text{-p-cym})\text{Ru}(\kappa^2\text{-O,O'-X})(\kappa^1\text{-P-L})\text{Y}]$ (where X = β -diketonate, L = dpim; PPh₂py; Y = BPh₄, BF₄) and also describe the *in vitro* anticancer activity of these compounds. In addition, we have examined the interaction of the new complexes with DNA. The main objectives of this work were to compare the role of the aforementioned aminophosphines in the biological properties of Ru(II) complexes and to establish a relationship between cytotoxic activity and DNA interaction. Indeed, it was found that the most active specimens are those that have the highest degree of interaction with the nucleic acid, namely $[(\eta^6\text{-p-cymene})\text{Ru}(\text{bzac})(\text{PPh}_2\text{py})]\text{BF}_4$ (bzac = benzoyl acetate) and $[(\eta^6\text{-p-cymene})\text{Ru}(\text{dbzm})(\text{PPh}_2\text{py})]\text{BF}_4$ (dbzm = dibenzoyl methanoate).

We also established a relationship between the hydrolysis rate of the new derivatives and the electronic features of the phosphine ligand and this could explain the observed cytotoxicity trends.

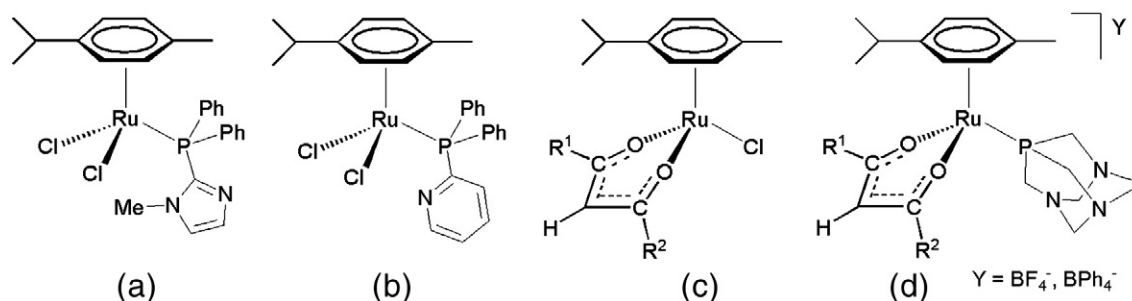
2. Experimental

2.1. Materials and reagents

Starting materials: $[(\eta^6\text{-p-cymene})\text{Ru}(\mu\text{-Cl})\text{Cl}]_2$, [25,26] dpim, [27] $[(\eta^6\text{-p-cymene})\text{Ru}(\text{acac})\text{Cl}]$ (**1**), [23] $[(\eta^6\text{-p-cymene})\text{Ru}(\text{bzac})\text{Cl}]$ (**2**), [28,29] $[(\eta^6\text{-p-cymene})\text{Ru}(\text{dbzm})\text{Cl}]$ (**3**), [24] and $[(\eta^6\text{-p-cymene})\text{Ru}(\text{hfacac})\text{Cl}]$ (**4**) [24] were prepared according to literature procedures. PPh₂py, acetylacetone (acacH), phenyl-1,3-butanedione (bzacH), 1,3-diphenyl-1,3-propanedione (dbzmH), hexafluoroacetylacetone (hfacH), NaBF₄, and NaBPh₄, were purchased from Aldrich and used without further purification. Deuterated solvents were obtained from SDS and Euriso-top. pBR322 plasmid DNA used in the EM and AFM studies was purchased from Boehringer Mannheim (Germany). Ultrapure agarose was obtained from ECOGEN (Barcelona, Spain). HEPES (N-2-hydroxyethyl piperazine-*N'*-2-ethanesulfonic acid) was obtained from ICN (Madrid). EDTA and Tris-HCl used in EM study were obtained from Sigma-Aldrich (Madrid, Spain).

2.2. General methods

All synthetic manipulations were carried out under an atmosphere of dry oxygen-free nitrogen using standard Schlenk techniques. Solvents were distilled from the appropriate drying agents and degassed before use. Elemental analyses were performed with a Perkin-Elmer 2400 CHN microanalyzer. The analytical data for the new complexes were obtained from crystalline samples when possible. In some cases the data were acceptably accurate, but in others the agreement of calculated and found values for carbon was >0.4%, so that solvent molecules were introduced in the molecular formulae to improve agreement. In any case, all the complexes were obtained in enough analytic purity to be used as starting materials. IR spectra were recorded on a Nicolet Impact 410 spectrophotometer as KBr pellets and on a Jasco (650–160 cm⁻¹ range) as Nujol mulls deposited on a polyethylene film. Only relevant bands are collected. The intensity of the peaks is described as: w = weak, m = medium, s = strong, vs = very strong. Fast atom bombardment mass (FAB MS) spectra (position of the peaks in DA) were recorded with an Autospec spectrometer. NMR spectra were recorded at 298 K (unless otherwise stated), on a Varian Unity Inova-400 (400 MHz for ¹H; 161.9 MHz for ³¹P; 100.6 MHz for ¹³C; 376 MHz for ¹⁹F MHz). ¹H and ¹³C{¹H} chemical shifts were internally referenced to TMS via the residual ¹H and ¹³C signals of CDCl₃ (δ = 7.26 ppm and δ = 77.36 ppm), according to the values reported by Fulmer et al. [30]. Chemical shift values are reported in ppm and coupling constants (J) in Hz. The splitting of proton resonances is defined as s = singlet, d = doublet, t = triplet, q = quartet, sept = septet, m = multiplet, bs = broad singlet. All ³¹P resonances were referenced to 85% H₃PO₄ at 0 ppm. 2D NMR spectra were recorded using standard pulse–pulse sequences: COSY (COrrrelation Spectroscopy), NOESY (Nuclear



Scheme 1. Structures of $[(\eta^6\text{-p-cym})\text{RuCl}_2(\kappa^1\text{-P-L})]$ (L = dpim, **A**; or PPh₂py, **B**), $[(\eta^6\text{-p-cym})\text{Ru}(\kappa^2\text{-O,O'-X})\text{Cl}]$ (**C**) and $[(\eta^6\text{-p-cym})\text{Ru}(\kappa^2\text{-O,O'-X})(\text{PTA})\text{Y}]$ (**D**).

Overhauser Enhancement Spectroscopy), HMQC (Heteronuclear Multiple Quantum Coherence), HMBC (Heteronuclear Multiple Bond Correlation). The probe temperature (± 1 K) was controlled by a standard unit calibrated with a methanol reference. All NMR data processing was carried out using MestReNova version 6.1.1.

Cyclic voltammetric (CV) experiments were performed in a J-Cambria ICH-660 potentiostat using a three electrode cell. Glassy carbon disk electrodes (3 mm diameter) from BAS were used as working electrodes, platinum wire as auxiliary and SSCE (Silver/Silver Chloride Electrode) as the reference electrode. Cyclic voltammograms were recorded at 100 mV/s scan rate. The complexes were dissolved in the corresponding solvents (dichloromethane or acetonitrile) containing the necessary amount of supporting electrolyte ((n-Bu₄N)(PF₆), TBAH) to yield a 0.1 M ionic strength solution.

2.3. X-ray crystallography

The single crystals for **1a**·BF₄, **1a**·BPh₄, **1b**·BPh₄, **2**, **3a**·BF₄ and **3b**·BPh₄ were mounted on a glass fiber and transferred to a Bruker X8 APEX II CCD-based diffractometer equipped with a graphite monochromated MoK α radiation source ($\lambda = 0.71073$ Å). The highly redundant datasets were integrated using SAINT [31] and corrected for Lorentz and polarization effects. The absorption correction was based on fitting a function to the empirical transmission surface as sampled by multiple equivalent measurements with the program SADABS [32].

The software package SHELXTL version 6.10 [33] was used for space group determination, structure solution and refinement by full-matrix least-squares methods based on F^2 . A successful solution by the direct methods provided most non-hydrogen atoms from the E-map. The remaining non-hydrogen atoms were located in an alternating series of least-squares cycles and difference Fourier maps. All non-hydrogen atoms were refined with anisotropic displacement coefficients unless specified otherwise. Hydrogen atoms were placed using a “riding model” and included in the refinement at calculated positions.

For compound **1b**·BPh₄, only crystals of low quality ($R_{int} = 0.226$) could be grown. Because of the weak diffraction, reflections have been included only up to $\theta = 21.0^\circ$ for the refinement and the data were refined isotropically only to reveal atomic connectivity. For complex **2**, the *p*-cymene ligand shows rotational disorder. In order to obtain chemically most reasonable results, the structure refinement was carried out with idealized rigid rings for all phenyl rings. Each of these rings was idealized and refined in spatial position and orientation and in its size using AFIX 3 instructions of program SHELXL97.

CCDC 871855, CCDC 871856, CCDC 871857, CCDC 871858, CCDC 871859, CCDC 871860 contain the supplementary crystallographic data for this paper. These data can be obtained free of charge from the Cambridge Crystallographic Data Centre via www.ccdc.cam.ac.uk/data_request/cif.

2.4. Solubility and stability

The ruthenium compounds were soluble in DMSO and aqueous DMSO. The ruthenium complexes were found sufficiently stable in the solution phases used after 48 h, as evidenced by the ¹H and ³¹P NMR.

2.5. Cell lines

The human breast cancer cell line MCF-7 and the human pancreatic cancer cells CAPAN-1 were obtained from the American Tissue Culture Collection (ATCC, Rockville, MD, USA). The cells were maintained in Dulbecco's modified eagle's medium (DMEM) supplemented with 10% fetal bovine serum and 1% penicillin–streptomycin (GIBCO BRL,

Grand Island, NY) at 37 °C in a humidified atmosphere containing 5% CO₂. The cells were passaged two times per week.

2.6. Cytotoxicity assays

The cytotoxicity of the ruthenium complexes in MCF-7 cells and CAPAN-1 cells was evaluated by the MTT assay. Aliquots of 2000 MCF-7 cells and 7000 CAPAN-1 cells were seeded in 96-well plates and cultured for 48 h with DMEM medium + 10% FBS. Then, the cells were treated for 48 h at 37 °C with the different ruthenium compounds, freshly dissolved in DMSO and milli-Q water, and then serially diluted in complete culture medium at concentrations ranging from 0 μ M to 100 μ M (DMSO final concentration in the culture medium < 1%). Next, the treatments were removed and the cells were washed with PBS and incubated for 3 additional hours in the darkness with 100 μ L of fresh culture medium together with 10 μ L of MTT (3-(4,5-dimethylthiazol-2-yl)-2,5-diphenyltetrazolium bromide) (Sigma-Aldrich, St. Louis, MO, USA). The medium was then discarded and dimethyl sulfoxide (DMSO) (Sigma-Aldrich) was added to each well to dissolve the purple formazan crystals. Plates were agitated at room temperature for 10 min and the absorbance of each well was determined with an absorbance microplate reader (ELx800, BioTek, Winooski, USA) at a wavelength of 570 nm. Three replicates were determined for each treatment, and all complexes were tested at least in three independent experiments. For each treatment, the cell viability was determined as a percentage of the untreated control cells, by dividing the mean absorbance of the treatment by the mean absorbance of the untreated cells. The concentration that reduces cell viability by 50% (IC₅₀) was then established for each compound.

2.7. Electrophoretic mobility study in agarose gel

The pBR322 plasmid DNA was used for the experiments at a concentration of 0.25 μ g/ μ L. Stock solutions of the ruthenium complexes were freshly prepared at a concentration of 0.1 μ g/ μ L in milli-Q water with 5% DMSO to facilitate the dissolution of compounds. The samples, with a final volume of 20 μ L, were prepared by addition of aliquots of the complex solutions to the pBR322 DNA in TE buffer (50 mM NaCl, 10 mM tris-(hydroxymethyl)aminomethane hydrochloride (Tris-HCl), 0.1 mM H₄edta, pH 7.4). The final concentration of DNA was 0.035 μ g/ μ L and the input molar ratio (r_i) of the complex to nucleotide = 0.50. A sample of pBR322 DNA with TE buffer alone was used as negative control. The samples were incubated for 24 or 48 h at 37 °C, and then 4 μ L of loading buffer (6 \times) (10 mM Tris-HCl (pH 7.6), 0.03% bromophenol blue, 0.03% xylene cyanol, 60% glycerol and 60 mM EDTA) were added to aliquots of 20 μ L of each sample. The mixtures were electrophoresed in a 0.5% agarose gel in TBE buffer (Tris-borate-EDTA, 89 mM Tris-borate, 2 mM EDTA, pH 8.3) for 3.5 h at 25 V. Afterwards, the DNA was dyed with a ethidium bromide solution (0.5 μ g/mL in TBE) for 45 min and the DNA bands were visualized. For comparison purposes, cisplatin was evaluated under the same experimental conditions.

2.8. AFM

The pBR322 plasmid DNA at 0.25 μ g/ μ L concentration was used for the experiments. Stock solution (0.1 μ g/ μ L) of the complexes in milli-Q water with 6% DMSO was freshly prepared. Samples ($V_f = 40$ μ L) were prepared by diluting 1 μ L of DNA pBR322 and an appropriate aliquot of the stock solution ($r_i = 0.50$) in HEPES buffer (N-2-hydroxyethyl piperazine-N'-2-ethanesulfonic acid), 10 mM MgCl₂, pH = 7.4) (DMSO final concentration < 1%). The different solutions as well as milli-Q water were passed through 0.2 μ m FP030/3 filters (Scheicher&Schueell GmbH, Germany) to provide a clear background. The resulting solutions were incubated for 24 h or

48 h at 37 °C. The samples were imaged in a NANOSCOPE III MULTIMODE AFM (Digital Instrumentals Inc., Santa Barbara) operating in tapping mode.

2.9. Cell death assay

The cell death pathway (apoptosis or necrosis) induced by the ruthenium compounds was evaluated using the **3b·BF₄** complex which demonstrated the highest cytotoxic activity. To this end, exponentially growing CAPAN-1 cells were seeded in a twelve-well plate (5×10^5 cells/well) and cultured for 24 h with DMEM medium + 10% FBS. Then, the medium was removed and the cells were treated for 24 h with a **3b·BF₄** solutions around two and three times the IC₅₀ (10 and 20 μM) or with medium alone, as a negative control. Then, the cell death was evaluated using the Vibrant Apoptosis Assay Kit #2 (Invitrogen, Paisley, UK), according to the manufacturer's instructions. Cells were harvested, washed in cold PBS and in diluted in 1X annexin-binding buffer to 1×10^6 cells/mL. Subsequently, cells were stained with Annexin V and propidium iodide (PI) and analyzed by flow cytometry using a FACSCalibur flow cytometer (Becton Dickinson Immunocytometry Systems, San Jose, CA) equipped with the CellQuest™ software (Becton Dickinson). 10,000 cells were analyzed in each experiment.

2.10. Synthesis of $[(\eta^6\text{-}p\text{-cymene})\text{Ru}(\text{bzac})\text{Cl}]$ (**2**) [28,29]

A suspension of Na₂CO₃ (102 mg, 0.651 mmol, 2 equiv.) in acetone (20 mL) was prepared. 1-Phenyl-1,3-butanedione (bzacH) (106 mg, 0.651 mmol, 2 equiv.) and $[(\eta^6\text{-}p\text{-cymene})\text{RuCl}_2]$ (200 mg, 0.326 mmol, 1 equiv.) were added, and the mixture was stirred at room temperature for 3 h and then filtered. The solvent was removed under vacuum. The residue was extracted with CH₂Cl₂ (4 × 8 mL), and the filtrated solution was concentrated under vacuum to 5 mL. Then n-hexane was added (30 mL) and the mixture was cooled in the freezer to produce an orange solid. Yield: 191 mg (0.651 mmol, 68.0%).

2.11. Synthesis of novel cationic complexes of general formula $[(\eta^6\text{-}p\text{-cymene})\text{Ru}(\kappa^2\text{-O},\text{O}'\text{-X})(\text{L})\text{Y}]$

A procedure based on that described by Dyson et al. was followed [23]. A solution of the respective starting material (**1–3**) (0.1616, mmol) in a (1:1) mixture of degassed solvents (acetone, 10 mL and dichloromethane, 10 mL) was prepared. Then, the corresponding sodium salt (NaBF₄, 0.3232 mmol) or (NaBPh₄, 0.1616 mmol) and aminophosphine (dpim or PPh₂py) (0.1616 mmol) were added. The mixture was stirred and heated to reflux temperature with a hot plate and then was left to cool slowly with stirring for 15 min. The heating/cooling cycle was repeated three more times to make a total reaction time of 1 h. The solution was evaporated to dryness under vacuum, and the solid residue was extracted with CH₂Cl₂ (3 × 10 mL). The extracts were filtered to remove the NaCl and the solvent removed under vacuum again. The solid residue was dissolved in CH₂Cl₂ (5 mL) and ethyl acetate (40 mL) was added. The mixture was concentrated to ca. 10 mL. Finally hexane (60 mL) was added and the schlenk was introduced in the freezer. Yellow solids were obtained after filtration, which were dried under vacuum.

2.11.1. $[(\eta^6\text{-}p\text{-cymene})\text{Ru}(\text{acac})(\text{dpim})\text{BF}_4]$ (**1a·BF₄**)

$[(\eta^6\text{-}p\text{-cym})\text{RuCl}(\text{acac})]$ (80.0 mg, 0.216 mmol); NaBF₄ (48.3 mg, 0.440 mmol), dpim (69.1 mg, 0.260 mmol). Yield: 92 mg (0.13 mmol, 62.0%). FW (C₃₁H₃₆N₂PO₂RuBF₄) = 687.49 g/mol. Anal. calcd for C₃₁H₃₆N₂PO₂RuBF₄: C, 54.16; H, 5.28; N, 4.07. Found: C, 53.85; H, 5.156; N, 4.224. ¹H NMR (400 MHz, CDCl₃) δ = 7.54–7.38 (m, 8 H, H^{m,p}-Ph, H^{4',5'}-Im), 7.30–7.23 (m, 4 H, H^o-Ph), 5.88 (d, ³J_{HH} = 6.3 Hz, 2 H, H^{2,6}-cym), 5.69 (d, ³J_{HH} = 6.3 Hz, 2 H, H^{3,5}-cym), 4.70 (s, 1 H, H^a-acac), 2.98 (s, 3 H, Me-Im), 2.37 (sept, ³J_{HH} = 7.0 Hz,

1 H, H⁷-cym), 1.75 (s, 6 H, H^c-acac), 1.57 (s, 3 H, H¹⁰-cym), 1.17 (d, ³J_{HH} = 7.0 Hz, 6 H, H^{8,9}-cym) ppm. ¹³C{¹H} NMR (101 MHz, CDCl₃) δ = 188.80 (s, 2C, C^b-acac), 136.69 (d, ¹J_{PC} = 84.5 Hz, 1C, C^{2'}-Im), 132.08 (d, ²J_{PC} = 9.8 Hz, 4C, C^o-Ph), 131.68 (d, ⁴J_{PC} = 2.5 Hz, 2C, C^p-Ph), 131.51 (s, 1C, C^{4'}-Im), 129.33 (d, ³J_{PC} = 10.2 Hz, 4C, C^m-Ph), 128.71 (s, 1C, C^{5'}-Im), 128.26 (d, ¹J_{PC} = 45.2 Hz, 2C, Cⁱ-Ph), 109.92 (d, ¹J_{PC} = 1.9 Hz, 1C, C¹-cym), 101.13 (s, 1C, C^a-acac), 98.61 (s, 1C, C⁴-cym), 89.33 (d, ¹J_{PC} = 3.5 Hz, 2C, C^{3,5}-cym), 87.08 (d, ¹J_{PC} = 4.6 Hz, 2C, C^{2,6}-cym), 36.05 (s, 1C, N-Me), 30.58 (s, 1C, C⁷-cym), 27.50 (s, 2C, C^c-acac), 22.12 (s, 2C, C^{8,9}-cym), 16.64 (s, 1C, C¹⁰-cym) ppm. ³¹P{¹H} NMR (162 MHz, CDCl₃) δ = 11.43 (s, 1 P, κ¹-dpim) ppm. ¹⁹F NMR (376 MHz, CDCl₃) δ = -154.44 (s, ¹⁰B-F, BF₄⁻), -154.49 (s, ¹¹B-F, BF₄⁻) ppm. FT-IR (KBr, cm⁻¹): 3142, 3122, 3081 (ν_{CH, sp}), 2964 (ν_{CH, sp}), 1573 (s, ν_{C=O+C=C}), 1515 (s, ν_{C=C+C=O}), 1437 (ν_{P-C}), 1374 (δ_{s, Me}), 1281, 1054 (s, ν_{d B-F}), 750 (δ_{CH,oop}), 696 (m, δ_{C=C,oop}), 548 (m, dpim), 518 (dpim), 476 (dpim), 441, 421. MS (FAB+, CHCl₃): m/z (%) = 601 (34) [M-BF₄]⁺, 467 (18) [M-BF₄-cym]⁺, 335 (100) [M-BF₄-dpim]⁺. Molar Conductivity (CH₃CN): 121.3 S·cm²·mol⁻¹. Solubility: soluble in acetone, dichloromethane, chloroform, methanol, barely soluble in ethanol and insoluble in water.

2.11.2. $[(\eta^6\text{-}p\text{-cymene})\text{Ru}(\text{acac})(\text{dpim})\text{BPh}_4]$ (**1a·BPh₄**)

$[(\eta^6\text{-}p\text{-cym})\text{RuCl}(\text{acac})]$ (37.8 mg, 0.102 mmol); NaBPh₄ (37.6 mg, 0.110 mmol), dpim (28.4 mg, 0.107 mmol). Yield: 65 mg (0.071 mmol, 69.5%). FW (C₅₅H₅₆N₂PO₂RuB₄) = 919.91 g/mol. Anal. calcd for C₅₅H₅₆N₂PO₂RuB₄·2H₂O: C, 69.10; H, 6.33; N, 2.93. Found: C, 68.68; H, 6.36; N, 2.94. ¹H NMR (400 MHz, CDCl₃) δ = 7.45 (m, 2 H, H^p-Ph, dpim), 7.39 (m, 9 H, 8 H^o-BPh, H^{4'}-Im), 7.35 (m, 4 H, H^m-Ph, dpim), 7.20–7.13 (m, 4 H, H^o-Ph, dpim), 7.08 (d, ³J_{HH} = 0.9 Hz, 1 H, H^{5'}-Im), 7.00 (t, ³J_{HH} = 7.4 Hz, 8 H, H^m-BPh, BPh₄⁻), 6.85 (m, 4 H, H^p-BPh, BPh₄⁻), 5.65 (d, ³J_{HH} = 6.2 Hz, 2 H, H^{2,6}-cym), 5.39 (d, ³J_{HH} = 5.3 Hz, 2 H, H^{3,5}-cym), 4.66 (s, 1 H, H^a-acac), 2.74 (s, 3 H, Me-Im), 2.30 (sept, ³J_{HH} = 7.0 Hz, 1 H, H⁷-cym), 1.71 (s, 6 H, H^c-acac), 1.38 (s, 3 H, H¹⁰-cym), 1.13 (d, ³J_{HH} = 7.0 Hz, 6 H, H^{8,9}-cym). ¹³C NMR (101 MHz, CDCl₃) δ = 188.60 (s, 2C, C^b-acac), 164.45 (q, ¹J_{BC} = 49.3 Hz, 4C, Cⁱ-BPh), 136.51 (q, ²J_{BC} = 1.3 Hz, 8C, C^o-BPh), 136.51 (d, ¹J_{PC} = 84.6 Hz, 1C, C^{2'}-Im), 131.83 (d, ²J_{PC} = 9.8 Hz, 4C, C^o-Ph), 131.75 (d, ⁴J_{PC} = 2.9 Hz, 2C, C^p-Ph), 131.59 (s, 1C, C^{4'}-Im), 129.34 (d, ³J_{PC} = 10.1 Hz, 4C, C^m-Ph), 128.48 (s, 1C, C^{5'}-Im), 128.06 (d, ¹J_{PC} = 44.9 Hz, 2C, Cⁱ-Ph, dpim), 125.66 (q, ³J_{BC} = 2.7 Hz, 8C, C^m-BPh), 121.75 (s, 4C, C^o-BPh), 109.88 (s, 1C, C¹-cym), 101.02 (s, 1C, C^a-acac), 98.06 (s, 1C, C⁴-cym), 89.39 (d, ¹J_{PC} = 3.4 Hz, 2C, C^{3,5}-cym), 86.72 (d, ¹J_{PC} = 4.7 Hz, 2C, C^{2,6}-cym), 35.94 (s, 1C, N-Me), 30.53 (s, 1C, C⁷-cym), 27.55 (s, 2C, C^c-acac), 22.08 (s, 2C, C^{8,9}-cym), 16.54 (s, 1C, C¹⁰-cym). ³¹P{¹H} NMR (162 MHz, CDCl₃) δ = 10.89 (s, 1 P, κ¹-dpim) ppm. FT-IR (KBr pellet and nujol mull, cm⁻¹): 3120, 3101, 3056 (m, ν_{CH, sp}), 2997, 2984 (ν_{CH, sp}), 1576 (s, ν_{C=O+C=C}), 1520 (s, ν_{C=C+C=O}), 1482 (BPh₄⁻), 1437 (ν_{P-C}), 1374 (δ_{s, Me}), 1276, 1098 (m, ν_{P-C}), 1032 (m), 781 (m), 748 (m, δ_{CH,oop}), 733 (s), 704 (s, δ_{C=C,oop}, BPh₄⁻), 612 (m), 546 (m, dpim), 519 (dpim), 477 (dpim), 439 (w), 422 (w), 203 (w, Ru-P). MS (FAB+, CHCl₃): m/z (%) = 601 (23) [M-BPh₄]⁺, 467 (9) [M-BPh₄-cym]⁺, 335 (100) [M-BPh₄-dpim]⁺. Molar Conductivity (CH₃CN): 119.7 S·cm²·mol⁻¹. Solubility: soluble in acetone, dichloromethane, chloroform, barely soluble in methanol and ethanol and insoluble in water.

2.11.3. $[(\eta^6\text{-}p\text{-cymene})\text{Ru}(\text{bzac})(\text{dpim})\text{BF}_4]$ (**2a·BF₄**)

$[(\eta^6\text{-}p\text{-cym})\text{RuCl}(\text{bzac})]$ (80.8 mg, 0.185 mmol); NaBF₄ (40.9 mg, 0.373 mmol), dpim (52.5 mg, 0.197 mmol). Yield: 102.7 mg (0.137 mmol, 74 %). FW (C₃₆H₃₈N₂PO₂RuBF₄) = 749.56 g/mol. Anal. calcd for C₃₆H₃₈N₂PO₂RuBF₄: C 57.69; H 5.11; N 3.74; Found: C 57.57; H 4.95; N 3.79. ¹H NMR (400 MHz, CDCl₃) δ = 7.60–7.17 (m, 17 H, Ph, H^{4',5'}-Im), 6.04 (d, ³J_{HH} = 6.0 Hz, 1 H, H⁶-cym), 5.87 (d, ³J_{HH} = 6.0 Hz, 1 H, H²-cym), 5.81 (d, ³J_{HH} = 6.0 Hz, 1 H, H³-cym), 5.71 (d, ³J_{HH} = 6.0 Hz, 1 H, H⁵-cym), 5.38 (s, 1 H, H^a-bzac), 2.95 (s, 3 H, Me-Im), 2.42 (sept, ³J_{HH} = 7.0 Hz, 1 H, H⁷-cym), 1.89 (s, 3 H, Me-bzac), 1.64 (s, 3 H,

H¹⁰-cym), 1.23 (d, ³J_{HH} = 7.0 Hz, 3 H, H⁸-cym), 1.16 (d, ³J_{HH} = 7.0 Hz, 3 H, H⁹-cym) ppm. ¹³C{¹H} NMR (101 MHz, CDCl₃) δ = 190.54 (s, 2C, C^b-bzac), 181.21 (s, 2C, C^b-bzac), 137.30 (s, 2C, Cⁱ-Ph-bzac), 136.61 (d, ¹J_{PC} = 85.3 Hz, 1C, C²-Im), 132.17 (d, ²J_{PC} = 9.8 Hz, 2C, C^o-Ph-dpim), 132.13 (d, ²J_{PC} = 9.8 Hz, 2C, C^o-Ph-dpim), 131.88 (s, 1C, C^p-Ph-bzac), 131.73 (d, ⁴J_{PC} = 2.1 Hz, 1C, C^p-Ph-dpim), 131.68 (d, ⁴J_{PC} = 2.0 Hz, 1C, C^p-Ph-dpim), 131.50 (s, 1C, C⁴-Im), 129.47 (d, ³J_{PC} = 10.4 Hz, 2C, C^m-Ph-dpim), 129.34 (d, ³J_{PC} = 10.5 Hz, 2C, C^m-Ph-dpim), 128.77 (s, 1C, C⁵-Im), 128.71 (s, 2C, Ph-bzac), 128.30 (d, ¹J_{PC} = 44.9 Hz, 1C, Cⁱ-Ph), 127.77 (d, ¹J_{PC} = 45.7 Hz, 1C, Cⁱ-Ph), 127.08 (s, 2C, Ph-bzac), 110.11 (s, 1C, C¹-cym), 98.53 (s, 1C, C⁴-cym), 97.98 (s, 1C, C^a-bzac), 89.78 (d, J_{PC} = 3.6 Hz, 1C, C⁵-cym), 89.45 (d, J_{PC} = 3.3 Hz, 1C, C³-cym), 87.22 (s, 2C, C^{6,2}-cym), 36.04 (s, 1C, N-Me), 30.57 (s, 1C, C⁷-cym), 28.27 (s, 1C, Me-bzac), 22.50 (s, 2C, C⁹-cym), 21.87 (s, 2C, C⁸-cym), 16.86 (s, 1C, C¹⁰-cym) ppm. ³¹P{¹H} NMR (162 MHz, CDCl₃) δ = 11.51 (s, 1P, κ¹-dpim) ppm. ¹⁹F NMR (376 MHz, CDCl₃) δ = -154.44 (s, ¹⁰B-F, BF₄⁻), -154.49 (s, ¹¹B-F, BF₄⁻) ppm. FT-IR (KBr, cm⁻¹): 3060 (ν_{CH, sp}), 2963, 2926, 2870 (ν_{CH, sp}), 1588 (s, ν_{C=O+C=C}), 1556 (vs, ν_{C=O+C=C}), 1516 (vs, ν_{C=C+C=O}), 1488 (s, ν_{C=C+C=O}), 1450, 1438 (ν_{p-c}), 1374 (s, δ_{s, Me}), 1057 (s, ν_{d B-F}), 754 (δ_{CH, oop}), 698 (m, δ_{C=C, oop}), 547 (m, dpim), 518 (dpim), 477 (dpim), 439. MS (FAB+, CHCl₃): m/z (%) = 663 (22) [M-BF₄]⁺, 529 (7) [M-BF₄-cym]⁺, 397 (100) [M-BF₄-dpim]⁺. Molar conductivity (CH₃CN): 145.4 S·cm²·mol⁻¹. Solubility: soluble in acetone, methanol, ethanol, dichloromethane, chloroform and insoluble in water.

2.11.4. [(η⁶-p-cymene)Ru(bzac)(dpim)]BPh₄ (**2a-BPh₄**)

(η⁶-p-cym)RuCl(bzac) (100.1 mg, 0.231 mmol); NaBPh₄ (82.9 mg, 0.242 mmol), dpim (65.2 mg, 0.245 mmol). Yield: 200.1 mg (0.204 mmol, 88.2 %). FW (C₆₀H₅₈N₂PO₂RuB) = 981.98 g/mol. Anal. calcd for C₆₀H₅₈N₂PO₂RuB·2H₂O: C, 70.45; H, 5.68; N, 2.87. Found: C, 70.79; H, 6.14; N, 2.75. ³¹H NMR (400 MHz, CDCl₃) δ = 7.55–7.27 (m, 17 H, Ph), 7.20–7.04 (m, 8 H, Ph, H^{4',5'}-Im), 7.39 (m, 8 H, H^o-BPh), 6.98 (t, ³J = 7.4 Hz, 8 H, H^m-BPh), 6.83 (t, ³J = 7.2 Hz, 4 H, H^p-BPh), 5.80 (d, ³J_{HH} = 6.1 Hz, 1 H, H⁶-cym), 5.65 (d, ³J_{HH} = 6.0 Hz, 1 H, H²-cym), 5.49 (d, ³J_{HH} = 6.2 Hz, 1 H, H²-cym), 5.41 (d, ³J_{HH} = 6.1 Hz, 1 H, H⁵-cym), 5.35 (s, 1 H, H^a-bzac), 2.70 (s, 3 H, Me-Im), 2.34 (sept, ³J_{HH} = 7.0 Hz, 1 H, H⁷-cym), 1.84 (s, 3 H, Me-bzac), 1.45 (s, 3 H, H¹⁰-cym), 1.17 (d, ³J_{HH} = 6.9 Hz, 3 H, H⁸-cym), 1.12 (d, ³J_{HH} = 6.9 Hz, 3 H, H⁹-cym) ppm. ¹³C{¹H} NMR (101 MHz, CDCl₃) δ = 190.17 (s, 1C, C^b-bzac), 181.19 (s, 1C, C^b-bzac), 164.43 (q, ¹J_{CB} = 49.6 Hz, 4C, Cⁱ, BPh₄⁻), 137.25 (s, 1C, Cⁱ-Ph-bzac), 136.49 (s, 8C, C^o-Ph, BPh₄⁻), 136.49 (d, ¹J_{PC} = 80.4 Hz, 1C, C²-Im), 131.93 (d, ²J_{PC} = 9.8 Hz, 2C, C^o-Ph-dpim), 131.87 (d, ²J_{PC} = 9.8 Hz, 2C, C^o-Ph-dpim), 131.77 (s, 1C, C^p-Ph-bzac), 131.55 (s, 1C, C^p-Ph-dpim), 129.44 (d, ³J_{PC} = 10.4 Hz, 2C, C^m-Ph-dpim), 129.34 (d, ³J_{PC} = 10.3 Hz, 2C, C^m-Ph-dpim), 128.95 (s, 1C, C⁵-Im), 128.76 (s, 2C, C^m-Ph-bzac), 128.15 (d, ¹J_{PC} = 44.9 Hz, 1C, Cⁱ-Ph), 127.77 (d, ¹J_{PC} = 37.3 Hz, 1C, Cⁱ-Ph), 127.01 (s, 2C, Ph-bzac), 125.67 (m, 8C, C^m, BPh₄⁻), 109.68 (s, 1C, C¹-cym), 97.91 (s, 1C, C⁴-cym), 97.87 (s, 1C, C^a-bzac), 90.12 (d, J_{PC} = 3.5 Hz, 1C, C⁵-cym), 89.49 (d, J_{PC} = 3.3 Hz, 1C, C³-cym), 86.92 (s, 1C, C⁶-cym), 86.88 (s, 1C, C²-cym), 35.90 (s, 1C, N-Me), 30.50 (s, 1C, C⁷-cym), 28.31 (s, 1C, Me-bzac), 22.45 (s, 2C, C⁹-cym), 21.87 (s, 2C, C⁸-cym), 16.73 (s, 1C, C¹⁰-cym) ppm. C⁴-Im and one C^p-Ph-dpim could not be assigned. ³¹P{¹H} NMR (162 MHz, CDCl₃) δ = 10.85 (s, 1P, κ¹-dpim) ppm. FT-IR (KBr pellet and nujol mull, cm⁻¹): 3102 (w), 3055 (m, ν_{CH, sp}), 2984 (ν_{CH, sp}), 2966, 1588 (s, ν_{C=O+C=C}), 1556 (vs, ν_{C=O+C=C}), 1519 (vs, ν_{C=C+C=O}), 1486 (s, ν_{C=C+C=O}), 1437 (ν_{p-c}), 1372 (δ_{s, Me}), 1277, 1098 (m, ν_{p-c}), 1031 (m), 1000, 774 (m), 746 (m, δ_{CH, oop}), 734 (s), 703 (s, δ_{C=C, oop}), 613 (m), 547 (m, dpim), 518 (dpim), 477 (dpim), 439 (w), 258 (w), 227 (w), 189 (w, Ru-P). MS (FAB+, CHCl₃): m/z (%) = 663 (9) [M-BPh₄]⁺, 529 (5) [M-BPh₄-cym]⁺, 397 (100) [M-BPh₄-dpim]⁺. Molar conductivity (CH₃CN): 97.1 S·cm²·mol⁻¹.

Solubility: soluble in acetone, chloroform and dichloromethane, barely soluble in methanol and ethanol, and insoluble in water.

2.11.5. [(η⁶-p-cymene)Ru(dbzm)(dpim)]BF₄ (**3a-BF₄**)

(η⁶-p-cym)RuCl(dbzm) (80.3 mg, 0.162 mmol); NaBF₄ (35.5 mg, 0.323 mmol), dpim (45.5 mg, 0.162 mmol). Yield: 86.6 mg (0.107 mmol, 66.0%). FW (C₄₁H₄₀N₂PO₂RuBF₄) = 811.63 g/mol. Anal. calcd for C₄₁H₄₀N₂PO₂RuBF₄: C, 60.67; H, 4.97; N, 3.45. Found: C, 60.77; H, 4.95; N, 3.56. ¹H NMR (400 MHz, CDCl₃) δ = 7.63 (d, 4 H, H^o-Ph, dbzm), 7.52 (m, 2 H, H-Ph), 7.48–7.33 (m, 8 H, H-Ph), 7.27–7.16 (m, 6 H, H-Ph), 6.07 (s, 1 H, H^a-dbzm), 6.05 (d, ³J_{HH} = 6.2 Hz, 2 H, H^{2,6}-cym), 5.82 (d, ³J_{HH} = 5.9 Hz, 2 H, H^{3,5}-cym), 2.94 (s, 3 H, Me-Im), 2.50 (sept, ³J_{HH} = 7.0 Hz, 1 H, H⁷-cym), 1.71 (s, 3 H, H¹⁰-cym), 1.23 (d, ³J_{HH} = 7.0 Hz, 6 H, H^{8,9}-cym) ppm. ¹³C{¹H} NMR (101 MHz, CDCl₃) δ = 182.89 (s, 2C, C^b-dbzm), 137.80 (s, 2C, Cⁱ-Ph-dbzm), 136.56 (d, ¹J_{PC} = 42.0 Hz, 1C, C²-Im), 132.18 (d, ²J_{PC} = 9.9 Hz, 4C, C^o-Ph-dpim), 132.07 (s, 2C, C^o-Ph-dbzm), 131.69 (s, 1C, C⁴-Im), 131.52 (s, ⁴J_{PC} = 2.3 Hz, 2C, C^p-Ph-dpim), 129.45 (d, ³J_{PC} = 10.2 Hz, 4C, C^m-Ph-dpim), 128.82 (s, 4C, C^m-Ph-dbzm), 128.33 (s, 1C, C⁵-Im), 127.80 (d, ¹J_{PC} = 46.1 Hz, 2C, Cⁱ-Ph, dpim), 127.09 (s, 4C, C^o-Ph-dbzm), 110.46 (s, 1C, C¹-cym), 98.36 (s, 1C, C⁴-cym), 95.17 (s, 1C, C^a-dbzm), 89.91 (d, J_{PC} = 3.4 Hz, 2C, C^{3,5}-cym), 87.32 (d, J_{PC} = 4.9 Hz, 2C, C^{2,6}-cym), 36.02 (s, 1C, N-Me), 30.55 (s, 1C, C⁷-cym), 22.24 (s, 2C, C^{8,9}-cym), 17.07 (s, 1C, C¹⁰-cym) ppm. ³¹P{¹H} NMR (162 MHz, CDCl₃) δ = 11.44 (s, 1P, κ¹-dpim) ppm. ¹⁹F NMR (376 MHz, CDCl₃) δ = -154.44 (s, ¹⁰B-F, BF₄⁻), -154.49 (s, ¹¹B-F, BF₄⁻) ppm. FT-IR (KBr, cm⁻¹): 3060 (ν_{CH, sp}), 2963, 2925 (ν_{CH, sp}), 1734, 1589 (m, ν_{C=O+C=C}), 1538 (vs, ν_{C=O+C=C}), 1520 (vs, ν_{C=C+C=O}), 1483 (s, ν_{C=C+C=O}), 1452, 1439 (ν_{p-c}), 1373 (s, δ_{s, Me}), 1084, 1059 (s, ν_{d B-F}), 1000, 752 (δ_{CH, oop}), 699 (m, δ_{C=C, oop}), 548 (m, dpim), 517 (dpim), 478 (dpim), 438. MS (FAB+, CHCl₃): m/z (%) = 725 (47) [M-BF₄]⁺, 591 (11) [M-BF₄-cym]⁺, 459 (100) [M-BF₄-dpim]⁺. Molar conductivity (CH₃CN): 145 S·cm²·mol⁻¹. Solubility: soluble in acetone, methanol, dichloromethane, chloroform, and barely soluble in ethanol, and insoluble in water.

2.11.6. [(η⁶-p-cymene)Ru(dbzm)(dpim)]BPh₄ (**3a-BPh₄**)

(η⁶-p-cym)RuCl(dbzm) (77.6 mg, 0.157 mmol); NaBPh₄ (56.9 mg, 0.166 mmol), dpim (44.4 mg, 0.167 mmol). Yield: 135.6 mg (0.130 mmol, 82.8 %). FW (C₆₅H₆₀N₂PO₂RuB) = 1044.06 g/mol. Anal. calcd for C₆₅H₆₀N₂PO₂RuB·H₂O: C, 73.51; H, 5.88; N, 2.64. Found: C, 73.51; H, 5.49; N, 2.68. ¹H NMR (400 MHz, CDCl₃) δ = 7.59 (m, 4 H, H^o-Ph, dbzm), 7.53 (m, 2 H, H^p-Ph, dbzm), 7.45–7.31 (m, 14 H, H^m-Ph-dbzm, H^o-Ph-BPh, H^p-Ph-dpim), 7.17–7.05 (m, 10 H, H^o-Ph-dpim, H^{4',5'}-Im), 6.96 (t, ³J_{HH} = 7.4 Hz, 8 H, H^m-BPh, BPh₄⁻), 6.80 (t, ³J_{HH} = 7.4 Hz, 4 H, H^p-BPh, BPh₄⁻), 6.05 (s, 1 H, H^a-dbzm), 5.82 (d, ³J_{HH} = 6.3 Hz, 2 H, H^{2,6}-cym), 5.50 (d, ³J_{HH} = 6.3 Hz, 2 H, H^{3,5}-cym), 2.69 (s, 3 H, Me-Im), 2.41 (sept, ³J_{HH} = 6.9 Hz, 1 H, H⁷-cym), 1.49 (s, 3 H, H¹⁰-cym), 1.17 (d, ³J_{HH} = 6.9 Hz, 6 H, H^{8,9}-cym) ppm. ¹³C{¹H} NMR (101 MHz, CDCl₃) δ = 182.77 (s, 2C, C^b-dbzm), 164.44 (q, ¹J_{CB} = 49.2 Hz, 4C, Cⁱ-Ph, BPh₄⁻), 137.79 (s, 2C, Cⁱ-Ph-dbzm), 136.48 (s, 8C, C^o-Ph, BPh₄⁻), 135.91 (d, ¹J_{PC} = 41.7 Hz, 1C, C²-Im), 132.15 (s, 2C, C^p-Ph, dbzm), 131.9 (d, ²J_{PC} = 9.7 Hz, 4C, C^o-Ph-dpim), 131.55 (s, 1C, C⁴-Im), 131.53 (s, 2C, C^p-Ph-dpim), 129.44 (d, ³J_{PC} = 10.2 Hz, 4C, C^m-Ph-dpim), 128.83 (s, 4C, C^m-Ph-dbzm), 128.55 (s, 1C, C⁵-Im), 127.69 (d, ¹J_{PC} = 44.9 Hz, 2C, Cⁱ-Ph, dpim), 127.01 (s, 4C, C^o-Ph-dbzm), 125.65 (q, ³J_{CB} = 2.8 Hz, 8C, C^m-Ph, BPh₄⁻), 121.75 (s, 4C, C^p-Ph, BPh₄⁻), 109.82 (s, 1C, C¹-cym), 97.54 (s, 1C, C⁴-cym), 95.11 (s, 1C, C^a-dbzm), 90.28 (d, J_{PC} = 3.4 Hz, 2C, C^{3,5}-cym), 86.98 (d, J_{PC} = 4.8 Hz, 2C, C^{2,6}-cym), 35.85 (s, 1C, N-Me), 30.44 (s, 1C, C⁷-cym), 22.21 (s, 2C, C^{8,9}-cym), 16.91 (s, 1C, C¹⁰-cym) ppm. ³¹P{¹H} NMR (162 MHz, CDCl₃) δ = 10.82 (s, 1P, κ¹-dpim) ppm. FT-IR (KBr pellet and nujol mull, cm⁻¹): 3112 (w), 3054 (m, ν_{CH, sp}), 2999, 2982 (ν_{CH, sp}), 2923, 1589 (m, ν_{C=O+C=C}), 1537 (vs, ν_{C=O+C=C}), 1520 (vs, ν_{C=C+C=O}), 1484 (s, ν_{C=C+C=O}), 1451, 1437 (ν_{p-c}), 1373 (δ_{s, Me}), 1314 (m), 1281, 1231, 1184, 1099 (m, ν_{p-c}), 1029 (m), 766 (m), 749 (m, δ_{CH, oop}), 732

(s), 702 (s, $\delta_{C=C, \text{oop}}$, BPh_4^-), 614 (m), 548 (m, dpim), 519 (dpim), 477 (dpim), 439 (w), 437 (w), 209 (w, Ru-P). MS (FAB+, CHCl_3): m/z (%) = 725 (35) $[\text{M-BPh}_4]^+$, 591 (10) $[\text{M-BPh}_4\text{-cym}]^+$, 459 (100) $[\text{M-BPh}_4\text{-dpim}]^+$. Molar Conductivity (CH_3CN): $115.2 \text{ S}\cdot\text{cm}^2\cdot\text{mol}^{-1}$. Solubility: soluble in acetone, chloroform and dichloromethane, barely soluble in methanol and ethanol, and insoluble in water.

2.11.7. $[(\eta^6\text{-}p\text{-cymene})\text{Ru}(\text{acac})(\text{PPh}_2\text{py})]\text{BF}_4$ (**1b-BF₄**)

$[(\eta^6\text{-}p\text{-cym})\text{RuCl}(\text{acac})]$ (100.3 mg, 0.270 mmol); NaBF_4 (60.9 mg, 0.545 mmol), PPh_2py (75.0 mg, 0.286 mmol). Yield: 107.2 mg (0.157 mmol, 58.0%) FW ($\text{C}_{32}\text{H}_{35}\text{NPO}_2\text{RuBF}_4$) = 684.48 g/mol. Anal. calcd for $\text{C}_{32}\text{H}_{35}\text{NPO}_2\text{RuBF}_4$: C, 56.15; H, 5.15; N, 2.05. Decomposition prevented from getting a good analysis and a mass spectrum. ^1H NMR (400 MHz, CDCl_3) δ = 8.94 (m, 1 H, $\text{H}^6\text{-py}$), 7.76 (m, 1 H, $\text{H}^4\text{-py}$), 7.53–7.46 (m, 3 H, $\text{H}^p\text{-Ph}$, $\text{H}^5\text{-py}$), 7.45–7.36 (m, 8 H, $\text{H}^{\text{om}}\text{-Ph}$), 7.28 (m, 1 H, $\text{H}^3\text{-py}$), 5.71 (d, $^3J_{\text{HH}} = 6.2 \text{ Hz}$, 2 H, $\text{H}^{2,6}\text{-cym}$), 5.59 (d, $^3J_{\text{HH}} = 6.2 \text{ Hz}$, 2 H, $\text{H}^{3,5}\text{-cym}$), 4.76 (s, 1 H, $\text{H}^a\text{-acac}$), 2.43 (sept, $^3J_{\text{HH}} = 6.9 \text{ Hz}$, 1 H, $\text{H}^7\text{-cym}$), 1.88 (s, 3 H, $\text{H}^{10}\text{-cym}$), 1.68 (s, 6 H, $\text{H}^c\text{-acac}$), 1.16 (d, $^3J_{\text{HH}} = 6.9 \text{ Hz}$, 6 H, $\text{H}^{8,9}\text{-cym}$) ppm. $^{13}\text{C}\{^1\text{H}\}$ NMR (101 MHz, CDCl_3) δ = 188.63 (s, 2C, $\text{C}^b\text{-acac}$), 134.44 (d, $^2J_{\text{PC}} = 9.5 \text{ Hz}$, 4C, $\text{C}^o\text{-Ph}$), 131.62 (d, $^4J_{\text{PC}} = 2.3 \text{ Hz}$, 2C, $\text{C}^p\text{-Ph}$), 128.79 (d, $^3J_{\text{PC}} = 10.0 \text{ Hz}$, 4C, $\text{C}^m\text{-Ph}$), 107.92 (s, 1C, $\text{C}^1\text{-cym}$), 100.70 (s, 1C, $\text{C}^a\text{-acac}$), 98.76 (s, 1C, $\text{C}^4\text{-cym}$), 88.94 (d, $J_{\text{PC}} = 3.7 \text{ Hz}$, 2C, $\text{C}^{3,5}\text{-cym}$), 88.32 (d, $J_{\text{PC}} = 4.2 \text{ Hz}$, 2C, $\text{C}^{2,6}\text{-cym}$), 30.69 (s, 1C, $\text{C}^7\text{-cym}$), 27.31 (s, 2C, $\text{C}^c\text{-acac}$), 22.05 (s, 2C, $\text{C}^{8,9}\text{-cym}$), 17.23 (s, 1C, $\text{C}^{10}\text{-cym}$) ppm. Some peaks could not be assigned due to low solubility and incipient decomposition as shown by appearance of free *p*-cym signals. $^{31}\text{P}\{^1\text{H}\}$ NMR (162 MHz, CDCl_3) δ = 28.94 (s, 1P, $\kappa^1\text{-PPh}_2\text{py}$) ppm. ^{19}F NMR (376 MHz, CDCl_3) δ = -154.45 (s, $^{10}\text{B-F}$, BF_4^-), -154.51 (s, $^{11}\text{B-F}$, BF_4^-) ppm. FT-IR (KBr, cm^{-1}): 3056 ($\nu_{\text{CH, sp}}$), 2960, 2921, 2869 ($\nu_{\text{CH, sp}}$), 1574 (s, $\nu_{\text{C=O+C=C}}$), 1517 (s, $\nu_{\text{C=C+C=O}}$), 1436 ($\nu_{\text{P-C}}$), 1378 ($\delta_{\text{s, Me}}$), 1276, 1058 (s, $\nu_{\text{d B-F}}$), 744 ($\delta_{\text{CH,oop}}$), 696 ($\delta_{\text{C=C, oop}}$), 529 (PPh_2py), 511 (PPh_2py), 448. Solubility: soluble in acetone, dichloromethane and chloroform, and insoluble in water.

2.11.8. $[(\eta^6\text{-}p\text{-cymene})\text{Ru}(\text{acac})(\text{PPh}_2\text{py})]\text{BPh}_4$ (**1b-BPh₄**)

$[(\eta^6\text{-}p\text{-cym})\text{RuCl}(\text{acac})]$ (99.8 mg, 0.270 mmol); NaBPh_4 (97.3 mg, 0.284 mmol), PPh_2py (75.8 mg, 0.288 mmol). Yield: 202.3 mg (0.220 mmol, 81.5 %) FW ($\text{C}_{56}\text{H}_{55}\text{NPO}_2\text{RuB}$) = 916.91 g/mol. Anal. calcd for $\text{C}_{56}\text{H}_{55}\text{NPO}_2\text{RuB}\cdot 2\text{H}_2\text{O}$: C, 70.58; H, 6.24; N, 1.47. Found: C, 70.47; H, 5.83; N, 1.64. ^1H NMR (400 MHz, CDCl_3) δ = 8.81 (m, 1 H, $\text{H}^6\text{-py}$), 7.54 (m, 1 H, $\text{H}^4\text{-py}$), 7.48 (m, 2 H, $\text{H}^p\text{-PPh}$), 7.40 (m, 8 H, $\text{H}^o\text{-Ph}$, BPh_4^-), 7.37–7.28 (m, 9 H, $\text{H}^{\text{om}}\text{-PPh}$, $\text{H}^5\text{-py}$), 7.13 (m, 1 H, $\text{H}^3\text{-py}$), 6.98 (t, $^3J_{\text{HH}} = 7.2 \text{ Hz}$, 8 H, $\text{H}^m\text{-Ph}$, BPh_4^-), 6.84 (t, $^3J_{\text{HH}} = 7.2 \text{ Hz}$, 4 H, $\text{H}^p\text{-Ph}$, BPh_4^-), 5.36 (d, $^3J_{\text{HH}} = 6.2 \text{ Hz}$, 2 H, $\text{H}^{2,6}\text{-cym}$), 5.13 (d, $^3J_{\text{HH}} = 6.2 \text{ Hz}$, 2 H, $\text{H}^{3,5}\text{-cym}$), 4.73 (s, 1 H, $\text{H}^a\text{-acac}$), 2.33 (sept, $^3J_{\text{HH}} = 7.0 \text{ Hz}$, 1 H, $\text{H}^7\text{-cym}$), 1.65 (s, 6 H, $\text{H}^c\text{-acac}$), 1.63 (s, 3 H, $\text{H}^{10}\text{-cym}$), 1.09 (d, $^3J_{\text{HH}} = 7.0 \text{ Hz}$, 6 H, $\text{H}^{8,9}\text{-cym}$) ppm. $^{13}\text{C}\{^1\text{H}\}$ NMR (101 MHz, CDCl_3) δ = 188.47 (s, 2C, $\text{C}^b\text{-acac}$), 164.46 (q, $^1J_{\text{PC}} = 49.2 \text{ Hz}$, 4C, $\text{C}^i\text{-BPh}$, BPh_4^-), 156.56 (d, $^1J_{\text{PC}} = 72.03 \text{ Hz}$, 1C, $\text{C}^{2\prime}\text{-py}$), 150.75 (d, $^3J_{\text{PC}} = 17.6 \text{ Hz}$, 1C, $\text{C}^{6\prime}\text{-py}$), 136.71 (d, $^3J_{\text{PC}} = 6.3 \text{ Hz}$, 1C, $\text{C}^{4\prime}\text{-py}$), 136.51 (s, 8C, $\text{C}^o\text{-BPh}$, BPh_4^-), 134.31 (d, $^2J_{\text{PC}} = 9.6 \text{ Hz}$, 4C, $\text{C}^o\text{-Ph}_2\text{P}$), 131.68 (d, $^4J_{\text{PC}} = 2.5 \text{ Hz}$, 2C, $\text{C}^p\text{-Ph}_2\text{P}$), 129.20 (d, $^2J_{\text{PC}} = 17.1 \text{ Hz}$, 1C, $\text{C}^{3\prime}\text{-py}$), 128.79 (d, $^3J_{\text{PC}} = 10.0 \text{ Hz}$, 4C, $\text{C}^m\text{-Ph}_2\text{P}$), 128.36 (d, $^1J_{\text{PC}} = 43.6 \text{ Hz}$, 2C, $\text{C}^i\text{-Ph}_2\text{P}$), 125.69 (q, $^3J_{\text{BC}} = 2.7 \text{ Hz}$, 8C, $\text{C}^m\text{-BPh}$, BPh_4^-), 125.34 (d, $^4J_{\text{PC}} = 2.3 \text{ Hz}$, 1C, $\text{C}^{5\prime}\text{-py}$), 107.56 (s, 1C, $\text{C}^1\text{-cym}$), 101.27 (s, 1C, $\text{C}^a\text{-acac}$), 98.01 (s, 1C, $\text{C}^4\text{-cym}$), 88.97 (d, $J_{\text{PC}} = 3.8 \text{ Hz}$, 2C, $\text{C}^{3,5}\text{-cym}$), 87.89 (d, $J_{\text{PC}} = 4.3 \text{ Hz}$, 2C, $\text{C}^{2,6}\text{-cym}$), 30.60 (s, 1C, $\text{C}^7\text{-cym}$), 27.32 (s, 2C, $\text{C}^c\text{-acac}$), 21.98 (s, 2C, $\text{C}^{8,9}\text{-cym}$), 17.09 (s, 1C, $\text{C}^{10}\text{-cym}$) ppm. $^{31}\text{P}\{^1\text{H}\}$ NMR (162 MHz, CDCl_3) δ = 28.61 (s, 1P, $\kappa^1\text{-PPh}_2\text{py}$) ppm. FT-IR (KBr pellet and nujol mull, cm^{-1}): 3055 (m), 2999, 2983 (w), 2969, 1573 (s, $\nu_{\text{C=O+C=C}}$), 1518 (s, $\nu_{\text{C=C+C=O}}$), 1480 (BPh_4^-), 1434 ($\nu_{\text{P-C}}$), 1372 ($\delta_{\text{s, Me}}$), 1275, 1097 (m, $\nu_{\text{P-C}}$), 1032 (m), 743 (m, $\delta_{\text{CH,oop}}$), 733 (s), 707 (s, $\delta_{\text{C=C, oop}}$, BPh_4^-), 614 (m), 533 (m, PPh_2py), 514 (PPh_2py), 482 (m), 470 (w), 443 (w), 432, 420, 210 (w, Ru-P), 188. MS (FAB+, CHCl_3): m/z (%) = 598 (11) $[\text{M-BPh}_4]^+$, 464

(7) $[\text{M-BPh}_4\text{-cym}]^+$, 335 (100) $[\text{M-BF}_4\text{-PPh}_2\text{py}]^+$. Molar conductivity (CH_3CN): $105.3 \text{ S}\cdot\text{cm}^2\cdot\text{mol}^{-1}$. Solubility: soluble in acetone, chloroform and dichloromethane, barely soluble in methanol and ethanol, and insoluble in water.

2.11.9. $[(\eta^6\text{-}p\text{-cymene})\text{Ru}(\text{bzac})(\text{PPh}_2\text{py})]\text{BF}_4$ (**2b-BF₄**)

$[(\eta^6\text{-}p\text{-cym})\text{RuCl}(\text{bzac})]$ (79.3 mg, 0.183 mmol); NaBF_4 (41.4 mg, 0.377 mmol), PPh_2py (51.8 mg, 0.197 mmol). Yield: 94.7 mg (0.127 mmol, 68.5%). FW ($\text{C}_{37}\text{H}_{37}\text{NPO}_2\text{RuBF}_4$) = 746.55 g/mol. Anal. calcd for $\text{C}_{37}\text{H}_{37}\text{NPO}_2\text{RuBF}_4\cdot 0.5\text{H}_2\text{O}$: C, 58.82; H, 5.07; N, 1.85. Found: C, 58.81; H, 4.60; N, 2.12. ^1H NMR (400 MHz, CDCl_3) δ = 8.90 (m, 1 H, $\text{H}^6\text{-py}$), 7.72 (m, 1 H, $\text{H}^4\text{-py}$), 7.59–7.22 (m, 17 H, $\text{H}^{3,5}\text{-py}$, Ph), 5.83 (d, $^3J_{\text{HH}} = 6.0 \text{ Hz}$, 1 H, $\text{H}^6\text{-cym}$), 5.68 (m, 2 H, $\text{H}^{3,2}\text{-cym}$), 5.65 (d, $^3J_{\text{HH}} = 6.0 \text{ Hz}$, 1 H, $\text{H}^5\text{-cym}$), 5.41 (s, 1 H, $\text{H}^a\text{-bzac}$), 2.47 (sept, $^3J_{\text{HH}} = 6.9 \text{ Hz}$, 1 H, $\text{H}^7\text{-cym}$), 1.96 (s, 3 H, $\text{H}^{10}\text{-cym}$), 1.82 (s, 3 H, Me-bzac), 1.18 (d, $^3J_{\text{HH}} = 6.9 \text{ Hz}$, 3 H, $\text{H}^8\text{-cym}$), 1.15 (d, $^3J_{\text{HH}} = 6.9 \text{ Hz}$, 3 H, $\text{H}^9\text{-cym}$) ppm. $^{13}\text{C}\{^1\text{H}\}$ NMR (101 MHz, CDCl_3) δ = 190.36 (s, 2C, $\text{C}^b\text{-bzac}$), 181.08 (s, 2C, $\text{C}^b\text{-bzac}$), 156.53 (d, $^1J_{\text{PC}} = 71.7 \text{ Hz}$, 1C, $\text{C}^{2\prime}\text{-py}$), 150.78 (d, $^3J_{\text{PC}} = 17.3 \text{ Hz}$, 1C, $\text{C}^{6\prime}\text{-py}$), 137.20 (s, 1C, $\text{C}^i\text{-bzac}$), 136.88 (d, $^3J_{\text{PC}} = 6.7 \text{ Hz}$, 1C, $\text{C}^{4\prime}\text{-py}$), 134.56 (d, $^2J_{\text{PC}} = 8.4 \text{ Hz}$, 2C, $\text{C}^o\text{-Ph}_2\text{P}$), 134.47 (d, $^2J_{\text{PC}} = 8.4 \text{ Hz}$, 2C, $\text{C}^o\text{-Ph}_2\text{P}$), 131.76 (s, 1C, $\text{C}^p\text{-bzac}$), 131.59 (d, $^4J_{\text{PC}} = 2.7 \text{ Hz}$, 1C, $\text{C}^p\text{-Ph}_2\text{P}$), 131.54 (d, $^4J_{\text{PC}} = 2.7 \text{ Hz}$, 1C, $\text{C}^p\text{-Ph}_2\text{P}$), 129.57 (d, $^2J_{\text{PC}} = 18.1 \text{ Hz}$, 1C, $\text{C}^{3\prime}\text{-py}$), 128.85 (d, $^3J_{\text{PC}} = 10.0 \text{ Hz}$, 2C, $\text{C}^m\text{-Ph}_2\text{P}$), 128.83 (d, $^3J_{\text{PC}} = 10.0 \text{ Hz}$, 2C, $\text{C}^m\text{-Ph}_2\text{P}$), 128.59 (s, 2C, $\text{C}^m\text{-bzac}$), 128.44 (d, $^1J_{\text{PC}} = 61.5 \text{ Hz}$, 1C, $\text{C}^i\text{-Ph}_2\text{P}$), 127.05 (s, 2C, $\text{C}^o\text{-bzac}$), 125.29 (d, $^4J_{\text{PC}} = 1.7 \text{ Hz}$, 1C, $\text{C}^{5\prime}\text{-py}$), 108.24 (d, $J_{\text{PC}} = 1.7 \text{ Hz}$, 1C, $\text{C}^1\text{-cym}$), 99.06 (s, 1C, $\text{C}^4\text{-cym}$), 98.18 (s, 1C, $\text{C}^a\text{-bzac}$), 89.05 (d, $J_{\text{PC}} = 3.6 \text{ Hz}$, 1C, CH-cym), 88.91 (d, $J_{\text{PC}} = 3.7 \text{ Hz}$, 1C, CH-cym), 88.65 (d, $J_{\text{PC}} = 4.1 \text{ Hz}$, 1C, CH-cym), 88.51 (d, $J_{\text{PC}} = 4.3 \text{ Hz}$, 1C, CH-cym), 30.70 (s, 1C, $\text{C}^7\text{-cym}$), 28.05 (s, 1C, Me-bzac), 22.48 (s, 1C, $\text{C}^9\text{-cym}$), 21.74 (s, 1C, $\text{C}^8\text{-cym}$), 17.44 (s, 1C, $\text{C}^{10}\text{-cym}$). The signal for one $\text{C}^i\text{-Ph}$ of PPh_2py is missed. $^{31}\text{P}\{^1\text{H}\}$ NMR (162 MHz, CDCl_3) δ = 29.02 (s, 1P, $\kappa^1\text{-P-PPh}_2\text{py}$) ppm. ^{19}F NMR (376 MHz, CDCl_3) δ = -153.98 (s, $^{10}\text{B-F}$, BF_4), -154.03 (s, $^{11}\text{B-F}$, BF_4^-) ppm. FT-IR (KBr, cm^{-1}): 3060 ($\nu_{\text{CH, sp}}$), 2964, 2927, 2872 ($\nu_{\text{CH, sp}}$), 1588 (s, $\nu_{\text{C=O+C=C}}$), 1556 (vs, $\nu_{\text{C=O+C=C}}$), 1515 (vs, $\nu_{\text{C=C+C=O}}$), 1487 (s, $\nu_{\text{C=C+C=O}}$), 1450, 1436 ($\nu_{\text{P-C}}$), 1376 ($\delta_{\text{s, CH}_3}$), 1058 (s, $\nu_{\text{d B-F}}$), 752 ($\delta_{\text{dCH,oop}}$), 697 (m, $\delta_{\text{C=C, oop}}$), 530 (m, PPh_2py), 514 (PPh_2py). MS (FAB+, CHCl_3): m/z (%) = 660 (31) $[\text{M-BF}_4]^+$, 526 (17) $[\text{M-BF}_4\text{-cym}]^+$, 397 (100) $[\text{M-BF}_4\text{-PPh}_2\text{py}]^+$. Molar conductivity (CH_3CN): $142.6 \text{ S}\cdot\text{cm}^2\cdot\text{mol}^{-1}$. Solubility: soluble in acetone, methanol, dichloromethane, chloroform and barely soluble in ethanol and insoluble in water.

2.11.10. $[(\eta^6\text{-}p\text{-cymene})\text{Ru}(\text{bzac})(\text{PPh}_2\text{py})]\text{BPh}_4$ (**2b-BPh₄**)

$[(\eta^6\text{-}p\text{-cym})\text{RuCl}(\text{bzac})]$ (99.7 mg, 0.230 mmol); NaBPh_4 (83.2 mg, 0.243 mmol), PPh_2py (64.9 mg, 0.247 mmol). Yield: 153.1 mg (0.156 mmol, 67.8%). FW ($\text{C}_{61}\text{H}_{57}\text{NPO}_2\text{RuB}$) = 978.98 g/mol. Anal. calcd for $\text{C}_{61}\text{H}_{57}\text{NPO}_2\text{RuB}\cdot 6\text{H}_2\text{O}$: C, 67.4; H, 6.40; N, 1.29. Found: C, 67.13; H, 5.82; N, 1.48. (bad correspondence, very hygroscopic complex). ^1H NMR (400 MHz, CDCl_3) δ = 8.78 (m, 1 H, $\text{H}^6\text{-py}$), 7.52 (m, 1 H, $\text{H}^4\text{-py}$), 7.48 (m, 4 H, $\text{H}^o\text{-PPh}$), 7.43–7.28 (m, 18 H, $\text{H}^o\text{-BPh}$, $\text{H}^m\text{-PPh}$, $\text{H}^5\text{-py}$, $\text{H}^{\text{om,p}}\text{-bzac}$), 7.23 (m, $\text{H}^p\text{-PPh}$), 7.10 (m, 1 H, $\text{H}^3\text{-py}$), 6.96 (t, $^3J_{\text{HH}} = 7.1 \text{ Hz}$, 8 H, $\text{H}^m\text{-BPh}$), 6.82 (t, $^3J_{\text{HH}} = 6.8 \text{ Hz}$, 4 H, $\text{H}^p\text{-BPh}$), 5.47 (d, $^3J_{\text{HH}} = 6.1 \text{ Hz}$, 1 H, $\text{H}^6\text{-cym}$), 5.41 (s, 1 H, $\text{H}^a\text{-bzac}$), 5.31 (d, $^3J_{\text{HH}} = 6.1 \text{ Hz}$, 1 H, $\text{H}^2\text{-cym}$), 5.20 (d, $^3J_{\text{HH}} = 6.1 \text{ Hz}$, 1 H, $\text{H}^5\text{-cym}$), 5.16 (d, $^3J_{\text{HH}} = 6.1 \text{ Hz}$, 1 H, $\text{H}^5\text{-cym}$), 2.36 (sept, $^3J_{\text{HH}} = 6.9 \text{ Hz}$, 1 H, $\text{H}^7\text{-cym}$), 1.78 (s, 3 H, Me-bzac), 1.69 (s, 3 H, $\text{H}^{10}\text{-cym}$), 1.11 (d, $^3J_{\text{HH}} = 6.9 \text{ Hz}$, 3 H, $\text{H}^8\text{-cym}$), 1.09 (d, $^3J_{\text{HH}} = 6.9 \text{ Hz}$, 3 H, $\text{H}^9\text{-cym}$) ppm. Acquisition of the $^{13}\text{C}\{^1\text{H}\}$ NMR failed due to low solubility and incipient decomposition. $^{31}\text{P}\{^1\text{H}\}$ NMR (162 MHz, CDCl_3) δ = 28.58 (s, 1P, $\kappa^1\text{-P-PPh}_2\text{py}$) ppm. FT-IR (KBr pellet and nujol mull, cm^{-1}): 3053 (m), 2997, 2981 (w), 2965, 1587 (s, $\nu_{\text{C=O+C=C}}$), 1553 (vs, $\nu_{\text{C=O+C=C}}$), 1519 (vs, $\nu_{\text{C=C+C=O}}$), 1486 (s, $\nu_{\text{C=C+C=O}}$), 1436 ($\nu_{\text{P-C}}$), 1371 ($\delta_{\text{s, Me}}$), 1289, 1097 (m, $\nu_{\text{P-C}}$), 1030 (m), 1000 (w), 853 (W), 770 (w), 744 (m, $\delta_{\text{CH,oop}}$), 734

(s), 705 (vs, $\delta_{C=C}$, oop, BPh_4^-), 613 (m), 526 (m, PPh_2py), 511 (PPh_2py), 502 (m), 460 (w), 445 (w), 420, 248, 212 (w, Ru-P), 188. MS (FAB+, $CHCl_3$): m/z (%) = 660 (22) $[M-BPh_4]^+$, 526 (11) $[M-BPh_4-cym]^+$, 397 (100) $[M-BPh_4-PPh_2py]^+$. Molar conductivity (CH_3CN): $100.4 S \cdot cm^2 \cdot mol^{-1}$. Solubility: soluble in acetone, chloroform and dichloromethane, barely soluble in methanol and ethanol, and insoluble in water.

2.11.11. $[(\eta^6-p-cymene)Ru(dbzm)(PPh_2py)]BF_4$ (**3b**·**BF₄**)

$[(\eta^6-p-cym)RuCl(dbzm)]$ (79.9 mg, 0.162 mmol); $NaBF_4$ (36.1 mg, 0.329 mmol), PPh_2py (45.0 mg, 0.171 mmol). Yield: 61.1 mg (0.076 mmol, 46.6%). FW ($C_{42}H_{39}NPO_2RuBF_4$) = 808.62 g/mol. Anal. calcd for $C_{42}H_{39}NPO_2RuBF_4$: C, 62.39; H, 4.86; N, 1.73. Found: C, 62.17; H, 4.69; N, 1.95. 1H NMR (400 MHz, $CDCl_3$) δ = 8.84 (m, 1 H, $H^{6'}$ -py), 7.67 (m, 1 H, $H^{4'}$ -py), 7.63–7.58 (m, 4 H, H^o -dbzm), 7.54–7.43 (m, 6 H, H^p -dbzm, H^o - PPh_2py), 7.43–7.37 (m, 7 H, $H^{5'}$ -py, H^m -dbzm, H^p - PPh_2py), 7.30–7.20 (m, 5 H, $H^{3'}$ -py, H^m - PPh_2py), 6.08 (s, 1 H, H^a -dbzm), 5.81 (d, $^3J_{HH}$ = 6.2 Hz, 2 H, $H^{2,6}$ -cym), 5.74 (d, $^3J_{HH}$ = 6.1 Hz, 2 H, $H^{3,5}$ -cym), 2.50 (sept, $^3J_{HH}$ = 6.9 Hz, 1 H, H^7 -cym), 2.02 (s, 3 H, H^{10} -cym), 1.18 (d, $^3J_{HH}$ = 6.9 Hz, 6 H, $H^{8,9}$ -cym) ppm. ^{13}C NMR (101 MHz, $CDCl_3$) δ = 182.75 (s, 2C, C^b -dbzm), 156.36 (d, $^1J_{PC}$ = 71.6 Hz, 1C, C^2 -py), 150.80 (d, $^3J_{PC}$ = 16.9 Hz, 1C, C^6 -py), 137.72 (s, 2C, C^i -dbzm), 136.91 (d, $^3J_{PC}$ = 6.9 Hz, 1C, C^4 -py), 134.57 (d, $^2J_{PC}$ = 9.7 Hz, 4C, C^o - Ph_2P), 131.94 (s, 2C, C^p -dbzm), 131.55 (d, $^4J_{PC}$ = 2.5 Hz, 2C, C^p - Ph_2P), 129.65 (d, $^2J_{PC}$ = 18.3 Hz, 1C, C^3 -py), 128.90 (d, $^3J_{PC}$ = 10.1 Hz, 4C, C^m - Ph_2P), 128.69 (s, 4C, C^m -dbzm), 128.51 (d, $^1J_{PC}$ = 45.1 Hz, 2C, C^i - Ph_2P), 127.07 (s, 4C, C^o -dbzm), 125.26 (d, $^4J_{PC}$ = 2.6 Hz, 1C, C^5 -py), 108.54 (s, 1C, C^1 -cym), 99.36 (s, 1C, C^4 -cym), 95.33 (s, 1C, C^a -dbzm), 88.95 (d, J_{PC} = 3.6 Hz, 2C, $C^{3,5}$ -cym), 88.82 (d, J_{PC} = 4.2 Hz, 2C, $C^{2,6}$ -cym), 30.69 (s, 1C, C^7 -cym), 22.18 (s, 2C, $C^{8,9}$ -cym), 17.67 (s, 1C, C^{10} -cym) ppm. ^{31}P NMR (162 MHz, $CDCl_3$) δ = 28.92 (s, 1P, κ^1 - PPh_2py) ppm. ^{19}F NMR (376 MHz, $CDCl_3$) δ = -154.44 (s, $^{10}B-F$, BF_4^-), -154.49 (s, $^{11}B-F$, BF_4^-) ppm. FT-IR (KBr, cm^{-1}): 3059 ($\nu_{CH, sp}$), 2964 ($\nu_{CH, sp}$), 1589 (m, $\nu_{C=O+C=C}$), 1571 ($\nu_{C=N}$), 1538, (vs, $\nu_{C=O+C=C}$), 1520 (vs, $\nu_{C=C+C=O}$), 1484 (s, $\nu_{C=C+C=O}$), 1452, 1437 (ν_{P-C}), 1374 (s, δ_s , CH_3), 1315, 1059 (s, ν_d B-F), 756 ($\delta_{CH,oop}$), 724, 696 (m, $\delta_{C=C, oop}$), 529 (m, PPh_2py), 514 (PPh_2py). MS (FAB+, $CHCl_3$): m/z (%) = 722 (22) $[M-BF_4]^+$, 588 (14) $[M-BF_4-cym]^+$, 459 (100) $[M-BF_4-PPh_2py]^+$. Molar conductivity (CH_3CN): $137.1 S \cdot cm^2 \cdot mol^{-1}$. Solubility: soluble in acetone, methanol, ethanol, dichloromethane and chloroform, and insoluble in water.

2.11.12. $[(\eta^6-p-cymene)Ru(dbzm)(PPh_2py)]BPh_4$ (**3b**·**BPh₄**)

$[(\eta^6-p-cym)RuCl(dbzm)]$ (80.0 mg, 0.160 mmol); $NaBPh_4$ (56.1 mg, 0.164 mmol), PPh_2py (45.2 mg, 0.172 mmol). Yield: 130.5 mg (0.125 mmol, 78.1%). FW ($C_{66}H_{59}NPO_2RuB$) = 1041.05 g/mol. Anal. calcd for $C_{66}H_{59}NPO_2RuB \cdot 3.5H_2O$: C, 71.8; H, 6.03; N, 1.27. Found: C, 71.74; H, 5.83; N, 1.40. 1H NMR (400 MHz, $CDCl_3$) δ = 8.72 (m, 1 H, $H^{6'}$ -py), 7.56 (m, 4 H, H^o -Ph, dbzm), 7.50 (m, 2 H, H^p -Ph, dbzm), 7.46 (m, 1 H, $H^{4'}$ -py), 7.42–7.32 (m, 18 H, H^o - PPh , H^o - BPh , H^m - CPh -dbzm), 7.26 (m, 1 H, $H^{5'}$ -py), 7.21 (m, 4 H, H^o - PPh), 7.05 (m, 1 H, $H^{3'}$ -py), 6.94 (t, $^3J_{HH}$ = 7.4 Hz, 8 H, H^m -Ph, BPh_4^-), 6.79 (t, $^3J_{HH}$ = 7.1 Hz, 4 H, H^p -Ph, BPh_4^-), 6.08 (s, 1 H, H^a -dbzm), 5.43 (d, $^3J_{HH}$ = 6.2 Hz, 2 H, $H^{2,6}$ -cym), 5.23 (d, $^3J_{HH}$ = 6.2 Hz, 2 H, $H^{3,5}$ -cym), 2.40 (sept, $^3J_{HH}$ = 6.9 Hz, 1 H, H^7 -cym), 1.74 (s, 3 H, H^{10} -cym), 1.11 (d, $^3J_{HH}$ = 6.9 Hz, 6 H, $H^{8,9}$ -cym) ppm. ^{13}C NMR (101 MHz, $CDCl_3$) δ = 182.74 (s, 2C, C^b -dbzm), 164.36 (q, $^1J_{BC}$ = 49.2 Hz, 4C, C^i - BPh , BPh_4^-), 156.56 (d, $^1J_{PC}$ = 72.03 Hz, 1C, C^2 -py), 150.62 (d, $^3J_{PC}$ = 17.6 Hz, 1C, C^6 -py), 137.70 (s, 2C, C^i -Ph-dbzm), 136.66 (d, $^3J_{PC}$ = 6.3 Hz, 1C, C^4 -py), 136.47 (s, 8C, C^o - BPh , BPh_4^-), 134.38 (d, $^2J_{PC}$ = 9.7 Hz, 4C, C^o - Ph_2P), 132.03 (s, 2C, C^p -Ph-dbzm), 131.61 (d, $^4J_{PC}$ = 2.5 Hz, 2C, C^p - Ph_2P), 129.24 (d, $^2J_{PC}$ = 17.1 Hz, 1C, C^3 -py), 128.89 (d, $^3J_{PC}$ = 9.8 Hz, 4C, C^m - Ph_2P), 128.72 (s, 4C, C^m -Ph-dbzm), 128.58 (d, $^1J_{PC}$ = 44.7 Hz, 2C, C^i - Ph_2P), 126.96 (s, 4C, C^o -Ph-dbzm), 125.67 (q, $^3J_{BC}$ = 2.7 Hz, 8C, C^m - BPh , BPh_4^-), 125.20 (d, $^4J_{PC}$ = 2.3 Hz, 1C, C^5 -py), 109.51 (s, 1C, C^1 -cym), 98.11 (s, 1C, C^a -dbzm), 95.41 (s, 1C, C^4 -cym), 89.41 (d, J_{PC} = 3.8 Hz, 2C,

$C^{3,5}$ -cym), 88.29 (d, J_{PC} = 4.3 Hz, 2C, $C^{2,6}$ -cym), 30.53 (s, 1C, C^7 -cym), 22.08 (s, 2C, $C^{8,9}$ -cym), 17.48 (s, 1C, C^{10} -cym) ppm. ^{31}P { 1H } NMR (162 MHz, $CDCl_3$) δ = 28.41 (s, 1P, κ^1 - PPh_2py) ppm. FT-IR (KBr pellet and nujol mull, cm^{-1}): 3055 (m), 2998, 2983 (w), 2966, 1588 (s, $\nu_{C=O+C=C}$), 1571 (w) 1538 (vs, $\nu_{C=O+C=C}$), 1520 (vs, $\nu_{C=C+C=O}$), 1483 (s, $\nu_{C=C+C=O}$), 1451, 1436 (ν_{P-C}), 1368 (δ_s , Me), 1314, 1230, 1183, 1097 (m, ν_{P-C}), 1030 (m), 1001 (w), 843 (W), 770 (w), 746 (m, $\delta_{CH,oop}$), 733 (s), 703 (vs, $\delta_{C=C, oop}$, BPh_4^-), 614 (m), 527 (m, PPh_2py), 512 (PPh_2py), 497 (m), 469 (w), 445 (w), 420, 280, 208 (w, Ru-P), 171. MS (FAB+, $CHCl_3$): m/z (%) = 722 (28) $[M-BPh_4]^+$, 588 (13) $[M-BPh_4-cym]^+$, 459 (100) $[M-BPh_4-PPh_2py]^+$. Molar conductivity (CH_3CN): $92.3 S \cdot cm^2 \cdot mol^{-1}$. Solubility: soluble in acetone, chloroform and dichloromethane, barely soluble in methanol and ethanol, and insoluble in water.

2.12. Computational studies

Computational modeling of the anion BPh_4^- and BF_4^- and single point calculation for the cation **1a**⁺ (using the structural data obtained from the X-ray crystallographic determination) were performed using the Gaussian 03 program [34], employing density functional theory with the hybrid method known as B3LYP, in which the Becke three-parameter exchange functional [35] and the Lee–Yang–Parr correlation functional were used [36]. For all nonmetal atoms, the contracted 6–31 G (d,p) [37,38] basis set was selected, which included diffuse functions. For the ruthenium center, the double- ζ basis set LanL2dz was used in conjunction with a pseudopotential representing the core set of electrons [39]. Structures of the anions were geometrically optimized to an energy minimum. The position on the local potential energy surface was confirmed through vibration analysis using second derivatives, where no imaginary frequencies were observed. The electrostatic potential maps, as shown in Fig. 5, were generated from the calculated electron density and potential using Gaussview [40].

The free energies of solvation were obtained using Barone and Cossi's implementation of the conductor like polarizable continuum model (C-PCM) [41,42]. The C-PCM calculations were performed with default parameters as single points on the gas-phase geometries since this has been shown to give better results than reoptimization [43]. The united atom topological model applied on atomic radii of the UFF force field (UA0) was used.

3. Results and discussion

3.1. Synthesis and general characterization

Precursors of formula $[(\eta^6-p-cym)Ru(\kappa^2-O,O'-X)Cl]$ **1–4** ($X = acac, bzac, dbzm, hfac$) were prepared according to the method described by Dyson et al. [23] in a one-pot reaction by treating a solution of $[(\eta^6-p-cymene)Ru(\mu-Cl)Cl]_2$ [26] in acetone with the appropriate 1,3-diketone and an excess of Na_2CO_3 at room temperature for approximately 3 h (see Scheme 2 and Eq. (1) in Scheme 3).

Novel complexes of general formula $[(\eta^6-p-cym)Ru(\kappa^2-O,O'-X)(\kappa^1-P-L)]Y$ ($X = acac, bzac, dbzm$), **1a**·**Y**–**3a**·**Y** and **1b**·**Y**–**3b**·**Y**, were prepared in acetone as BF_4^- or BPh_4^- salts by treatment of the corresponding precursors **1–3** with an excess of $NaBF_4$ or slight excess of $NaBPh_4$ and the corresponding phosphine: L = dpim for series a (**1a**·**Y**–**3a**·**Y**) and L = PPh_2py , for series b (**1b**·**Y**–**3b**·**Y**) (see Scheme 2 and Eq. (2) in Scheme 3). The complexes with bzac were obtained as racemic mixtures due to the chirality of the Ru ion. Attempts to prepare the corresponding analogues of **4** were unsuccessful. Complexes $[(\eta^6-p-cymene)RuCl(\kappa^2-P,N-L)]BF_4$ (**5a**·**BF₄** and **5b**·**BF₄**) were obtained instead, thus demonstrating that hfac behaves as a better leaving group than Cl^- under the conditions employed (see Eq. (3) in Scheme 3). Indeed, the weakness of the Ru–O bond in complex **4** has been reported previously [24].

All of the ionic complexes were isolated in moderate to good yields (from 47 to 88%) as yellow, orange or brown solids that were

air and moisture resistant – with the exception of **1b**·**BF₄**, which decomposed to give a dark solid in a few days under an air atmosphere. Qualitative tests indicated that the **BF₄**[−] salts are soluble in common organic solvents such as acetone, methanol, ethanol, chloroform and dichloromethane, whereas the **BPh₄**[−] derivatives are only soluble in dichloromethane, chloroform and acetone. Furthermore, neither of the salts is soluble in pure water despite being ionic, although **BF₄**[−] salts are soluble in H₂O/DMSO (98:2) mixtures. All of the compounds were comprehensively characterized on the basis of ¹H, ¹³C{¹H}, ¹⁹F (**BF₄**[−] salts) and ³¹P{¹H} NMR in CDCl₃, as well as by IR spectroscopy, positive ion FAB mass and elemental analysis. In addition, the solid state structures of **1a**·**BF₄**, **1a**·**BPh₄**, **3a**·**BF₄**, **1b**·**BPh₄** and **3b**·**BPh₄** were determined by X-ray diffraction.

FAB + mass spectra were acquired for all the new ionic complexes apart from **1b**·**BF₄**, which decomposed. Every spectrum contained a peak for the expected complex cation, [M – Y]⁺ (Y = **BF₄**[−] or **BPh₄**[−]), and two characteristic fragmentation peaks: (i) one for the loss of the *p*-cymene ring [M – Y – cym]⁺ and (ii) the base peak for the loss of the respective aminophosphine, [M – Y – L]⁺ (L = dpim or PPh₂py).

FT-IR spectra were recorded for all the complexes and are fully consistent with the aforementioned formulations. Complexes **1–4** show characteristic bands for the Ru–Cl stretching bands at around 280 cm^{−1} and these are not present in the cases of the cationic derivatives **1a**·**Y–3a**·**Y** and **1b**·**Y–3b**·**Y**. All of these spectra show the expected strong peaks for the **BF₄**[−] anion at around 1058 cm^{−1} and for the **BPh₄**[−] at around 704 cm^{−1} [21,44]. Moreover, the coupled ν_{C=O}+ν_{C=C} stretching peaks appear at characteristic values for each β-diketonate, i.e. around 1573 and 1515 cm^{−1} for acac, 1588, 1555, 1516 and 1488 cm^{−1} for bzac and finally 1589, 1538, 1520 and 1484 cm^{−1} for dbzm [28,29,45,46].

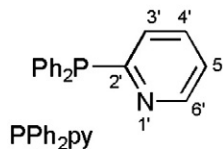
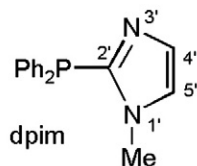
All of the **BF₄**[−] and **BPh₄**[−] salts behave as 1:1 electrolytes in acetonitrile solutions (10^{−3} M) according to the molar conductivity measurements (Λ_M) [47]. The values are clearly higher for the **BF₄**[−] salts (from

121.3 to 145.4) than for the **BPh₄**[−] salts (from 92.3 to 119.7) (see **Experimental** section and Table S6 of Supporting Information).

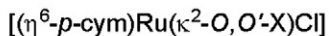
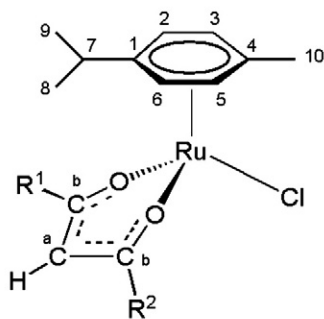
The ³¹P{¹H} NMR spectra of complexes **1a**·**Y–3a**·**Y** and **1b**·**Y–3b**·**Y** in CDCl₃ each contain one sharp singlet that is strongly shifted to higher frequency with respect to that for the corresponding free ligand. This shift is a consequence of coordination to the Ru ion (see **Table 1**). Indeed, the signals appear in a very narrow range, i.e. between 10.82 and 11.51 ppm for series a and from 28.41 to 29.02 ppm for series b. Interestingly, the ‘β-diketonate’ effect on δ (³¹P) is negligible in both series. By contrast, a weak but characteristic displacement to higher frequencies is observed for all of the **BF₄**[−] salts when compared to their **BPh₄**[−] counterparts, Δδ (³¹P) = 0.33–0.66, indicating that the donation of electron density from the phosphorus to the metal is slightly higher for **BF₄**[−] salts (**Table 1**). This counter-anion effect has been explained as being a consequence of a reduced bonding interaction between the arene ring and the Ru in the **BF₄** derivatives as compared to the **BPh₄** salts [23], and suggests that the counter-anions play a non-innocent role in the electronic system of the cationic complex. In any event, the recorded δ values compare well with those observed for the analogues [(η⁶-*p*-cym)RuCl₂(κ¹-*P*-L)] (L = dpim, **A**; or PPh₂py, **B** in **Scheme 1**) and they prove the κ¹-*P* coordination mode of the respective ligands [21,48,49]. Nevertheless, the resonances of the neutral complexes **A** and **B** appear at lower frequencies (meaning that the P atoms are more shielded) than those of their cationic β-diketonato relatives, **1a**·**Y–3a**·**Y** and **1b**·**Y–3b**·**Y**, and this finding could be due to the higher electronic density at the metal center in the former. The spectra of products **5a**·**BF₄** and **5b**·**BF₄** exhibit a singlet at −8.29 ppm and −16.54 ppm, respectively, and these are consistent with a κ²-*P,N* coordination mode for the corresponding ligands [21].

Complete assignment of the resonances in the ¹H and ¹³C{¹H} NMR spectra of all complexes for the corresponding arene, phosphine and β-diketonate was performed using 2D NMR experiments such as

Aminophosphines, L = Ph₂PR

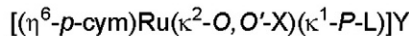
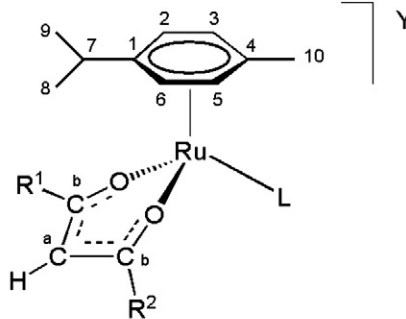


Ru(II) Precursors

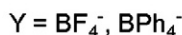


- 1: R¹ = R² = Me; X = acac
- 2: R¹ = Me; R² = Ph; X = bzac
- 3: R¹ = R² = Ph; X = dbzm
- 4: R¹ = R² = CF₃; X = hfac

Novel Ru(II) Complexes



- (**1a**·**Y–3a**·**Y**)
(**1b**·**Y–3b**·**Y**)



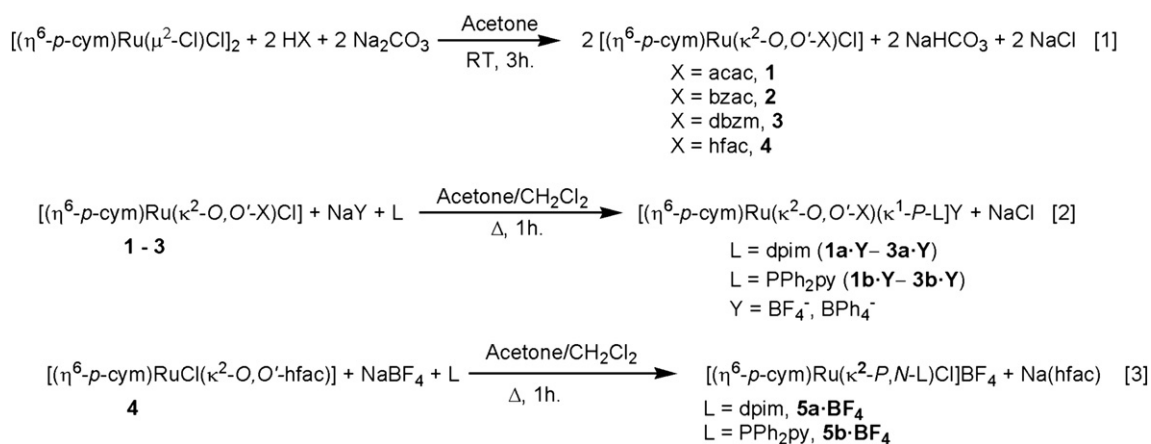
Series a: L = dpim

- 1a**·**BF₄** (X = acac)
1a·**BPh₄** (X = acac)
2a·**BF₄** (X = bzac)
2a·**BPh₄** (X = bzac)
3a·**BF₄** (X = dbzm)
3a·**BPh₄** (X = dbzm)

Series b: L = PPh₂py

- 1b**·**BF₄** (X = acac)
1b·**BPh₄** (X = acac)
2b·**BF₄** (X = bzac)
2b·**BPh₄** (X = bzac)
3b·**BF₄** (X = dbzm)
3b·**BPh₄** (X = dbzm)

Scheme 2. Structures and numbering of aminophosphine ligands, Ru(II) precursors of general formula [(η⁶-*p*-cymene)Ru(κ²-O, O'-X)Cl] and novel Ru(II) arene derivatives of general formula [(η⁶-*p*-cymene)Ru(κ²-O, O'-X)(κ¹-*P*-L)]Y reported in this work.



Scheme 3. Synthesis of the precursors **1–4** and the cationic complexes **1a·Y–3a·Y**, **1b·Y–3b·Y** (Y = BF₄[−], BPh₄[−]), **4a·BF₄** and **4b·BF₄**.

gCOSY, NOESY, gHSQC and gHMBC (see [Experimental](#) section and Table S7 of Supporting Information). The ¹H NMR spectra of complexes **1a·Y**, **3a·Y**, **1b·Y** and **3b·Y** reveal the local C_s symmetry of the metallic center (non-stereogenic and achirotopic in nature), with the characteristic AA'BB' spin system for the cymene aromatic protons and homotopic methyl groups for the isopropyl moiety [50]. On the other hand, the ¹H NMR spectra for complexes **2a·Y** and **2b·Y** display an ABCD spin system for the aromatic protons of the cymene ring and diastereotopic methyl groups in the isopropyl entity, which could indicate a C₁ symmetry environment for the stereogenic and chirotopic Ru ion [51]. The ¹³C{¹H} NMR spectra of all the complexes show symmetry patterns that are fully consistent with those established by ¹H NMR spectroscopy (see [Experimental](#) section).

The *p*-cymene aromatic protons in complexes **1a·Y–3a·Y** and **1b·Y–3b·Y** exhibit higher frequencies than those of the stable complexes [(η⁶-*p*-cym)RuCl₂(dpim)], **A**, and [(η⁶-*p*-cym)RuCl₂(PPh₂py)], **B**, respectively [21,48,49]. Such deshielding is similar to that of free *p*-cymene (7.13 ppm, multiplet, in CDCl₃) and could be interpreted as a symptom of weak coordination to the metallic center. In fact, free *p*-cymene was detected by ¹H and ¹³C{¹H} NMR spectroscopy in the corresponding samples (CDCl₃) of all the cationic complexes several hours after their preparation. The extent of decomposition in solution was estimated by the integration of ¹H NMR signals, which indicated less than 10% after 20 h in most cases. Exceptions to this behavior are **1a·BPh₄** and **3a·BPh₄**, which also decompose but at a slower rate. In particular, **1a·BPh₄**, as a model complex, was monitored over five days by ¹H and ³¹P{¹H} NMR spectroscopy in CDCl₃ and it was concluded that this compound undergoes a slow

and intricate evolution. Several emerging signals appeared in the ³¹P{¹H} NMR spectrum after 5 days (see [Fig. 1](#)). The ¹H NMR spectrum shows that 58% of **1a·BPh₄** remained unchanged along with 23% of free *p*-cymene and another unknown Ru-arene product. It is worth mentioning that both ring slippage and ring substitution processes have been alleged to operate as activation mechanisms in catalysis and also in reactions with potential biomolecular targets, including DNA [52–54].

Interestingly, the ¹H NMR spectra of the BPh₄[−] salts in CDCl₃ showed lower frequencies for all the resonances of the *p*-cymene and phosphine ligands in comparison to those recorded in the spectra of the BF₄[−] analogues. The effect is particularly pronounced for the aromatic *p*-cymene signals (e.g. 5.88 and 5.69 ppm for **1a·BF₄** and 5.65 and 5.40 ppm for **1a·BPh₄** in CDCl₃). This anion effect has been interpreted in similar complexes as evidence of stronger coordination of the *p*-cymene ring in the case of BPh₄[−] salts [23]. In our case, we ascribe this observation to the formation of specific ion-pairs, favored in solvents of low polarity such as CDCl₃, without detriment to the preceding argument. In particular, we propose that the *p*-cymene ring is involved in the formation of ion-pairs that differ in nature depending on the anion: (i) CH–π interactions involving aromatic CH groups of *p*-cymene and phenyl rings of the BPh₄[−] anion, with a shielding effect on the *p*-cymene NMR signals, and (ii) C–H···F hydrogen bonds, with a deshielding effect on the *p*-cymene NMR peaks, in the case of BF₄[−] salts. Such an interpretation is supported by the interionic contacts observed in the crystal structures determined by X-ray diffraction (see below).

In an effort to find evidence for the existence of ion-pairing we recorded the ¹H and ³¹P{¹H} NMR spectra for a mixture of **1a·BF₄**/**1a·BPh₄** (1:1) in CDCl₃. The proton resonances of this mixture showed average values between those of pure **1a·BF₄** and pure **1a·BPh₄** (see [Fig. 2](#)). This result is in accordance with a fast ionic exchange at room temperature and confirms the labile nature of these weak interactions. The ³¹P{¹H} NMR spectrum of the mixture produced a singlet at δ_P = 11.11 ppm, i.e. between those of pure **1a·BPh₄** (10.89 ppm) and pure **1a·BF₄** (11.43 ppm).

Comparison of the NMR data for the β-diketonate CH^α groups within the two sets of compounds (series a and series b) reveals some interesting trends. On the one hand, the ¹H NMR chemical shifts increase in the order acac < bzac < dbzm. On the other hand, the ¹³C NMR chemical shifts show the opposite trend and increase in the order dbzm < bzac < acac. It seems that the electron-donating Me group shields the H nucleus and deshields the C nucleus. In contrast, the electron-withdrawing Ph group deshields the proton and shields the carbon. These findings are consistent with the higher polarization of the C–H bond expected for the β-diketonates with electron-withdrawing groups.

Table 1

³¹P{¹H} NMR chemical shifts (ppm) for phosphines dpim and PPh₂py and complexes [(*p*-cym)Ru(X)(κ¹-P-L)] (L = dpim, **A**, **1a·Y–3a·Y**; L = PPh₂py, **B**, **1b·Y–3b·Y**) in CDCl₃ at 25 °C. All resonances were observed as singlets.

Series a	δ (ppm)	Δδ ^a	Series b	δ (ppm)	Δδ ^a
dpim	−29.47		PPh ₂ py	−7.63	
A	7.58		B	23.54	
1a·BF₄	11.43	0.54	1b·BF₄	28.94	0.33
1a·BPh₄	10.89		1b·BPh₄	28.61	
2a·BF₄	11.51	0.66	2b·BF₄	29.02	0.44
2a·BPh₄	10.85		2b·BPh₄	28.58	
3a·BF₄	11.44	0.62	3b·BF₄	28.92	0.51
3a·BPh₄	10.82		3b·BPh₄	28.41	

^a Δδ is the chemical shift difference for pairs of derivatives with identical cations and BF₄[−] or BPh₄[−] counter-ions.

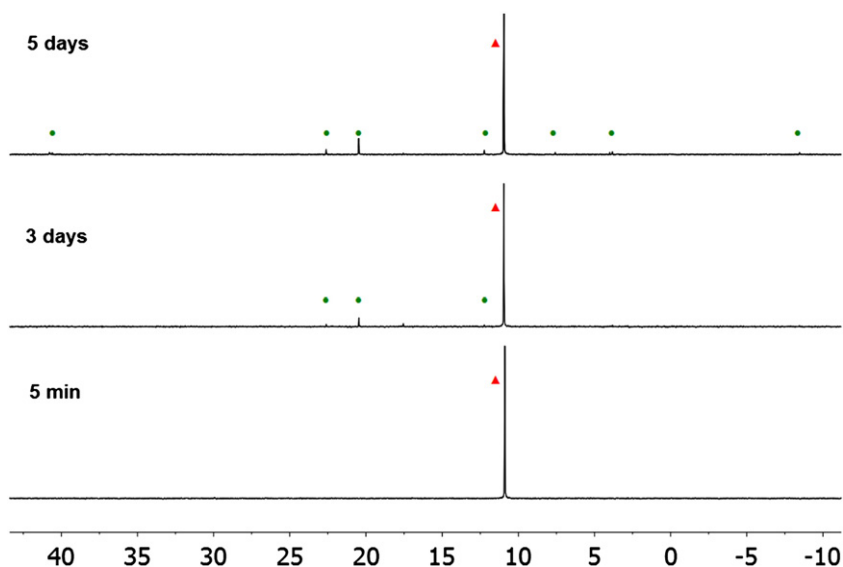


Fig. 1. Evolution with time of the $^{31}\text{P}\{^1\text{H}\}$ NMR spectrum for $1\mathbf{a}\cdot\text{BPh}_4$ (filled red triangle) in CDCl_3 . Evolution products are labelled as (filled green circle).

3.2. Solid state structures of $1\mathbf{a}\cdot\text{BF}_4$, $1\mathbf{a}\cdot\text{BPh}_4$, $3\mathbf{a}\cdot\text{BF}_4$, $1\mathbf{b}\cdot\text{BPh}_4$, $3\mathbf{b}\cdot\text{BPh}_4$ and 2

Single crystals suitable for X-ray analysis were obtained for $1\mathbf{a}\cdot\text{BF}_4$, $1\mathbf{a}\cdot\text{BPh}_4$, $3\mathbf{a}\cdot\text{BF}_4$, $1\mathbf{b}\cdot\text{BPh}_4$, $3\mathbf{b}\cdot\text{BPh}_4$ and 2 by either liquid–liquid diffusion techniques from $\text{CH}_2\text{Cl}_2/n\text{-hexane}$ ($1\mathbf{a}\cdot\text{BF}_4$), $\text{CH}_2\text{Cl}_2/n\text{-hexane}$ ($3\mathbf{b}\cdot\text{BPh}_4$), $\text{EtOH}/n\text{-hexane}$ ($3\mathbf{a}\cdot\text{BF}_4$) or by slow evaporation experiments from MeOH ($1\mathbf{a}\cdot\text{BPh}_4$) and acetonitrile ($1\mathbf{b}\cdot\text{BPh}_4$). Although complex 2 is not described in this paper for the first time, the determination of the structure by X-ray diffraction has not been reported and thus it is included in this section. Crystallization conditions are described in the **Experimental** section. The ORTEP diagrams are shown in Fig. 3. Unfortunately, the X-ray data obtained for $1\mathbf{b}\cdot\text{BPh}_4$ were of low quality. Nevertheless, the atom connectivity was defined sufficiently well to determine the important features of the structure. A ball and stick representation is depicted in Fig. 3. Relevant crystallographic parameters are listed in Table 2 and selected bond lengths and angles are given in Table 3.

The molecular structures fit the classical three-legged piano-stool arrangement with a pseudo-octahedral geometry and display similar molecular features to those of structurally related ruthenium complexes

[21,23]. The coordination sphere consists of a $\eta^6\text{-}p\text{-cymene}$ ring that occupies three facial coordination positions, plus the $\kappa^1\text{-}P\text{-phosphine}$ (chloride in the case of 2) and a $\kappa^2\text{-}O,O'\text{-}\beta\text{-diketonate}$. Ru–C(arene) bond distances are slightly different for each specific complex, with the shortest distances for those carbon atoms in a *cis* orientation to the P and the longest distances for those carbon atoms *trans* to the P, as one would expect according to the strongest *trans* influence of the phosphines in comparison to the O-donor ligands. For the aminophosphine derivatives with acac the range found for the Ru–C distances is 2.16–2.23 Å while for those containing dbzm it is 2.20–2.24 Å, i.e. a higher range is observed for complexes with acac than for those with dbzm. The Ru-arene centroid distance is slightly higher for the dbzm derivatives (1.70–1.71 Å) than for the acac complexes (1.69 Å). The values are very similar to those of the stable complexes [(*p*-cym)RuCl₂(dpim)], **A**, [1.700 Å] and [(*p*-cym)RuCl₂(PPh₂py)], **B**, [1.704 Å], for which loss of the *p*-cymene ring in solution has not been observed. Therefore, the possible weakness of the bond between the metal and the *p*-cymene observed for the novel $\beta\text{-diketonato}$ complexes in solution (partial loss of *p*-cymene in CDCl_3) does not seem to persist in the solid state. The Ru-arene centroid distance is smaller for 2 (1.655 Å), which is the only neutral derivative. The Ru–P bond lengths are in the range 2.34–

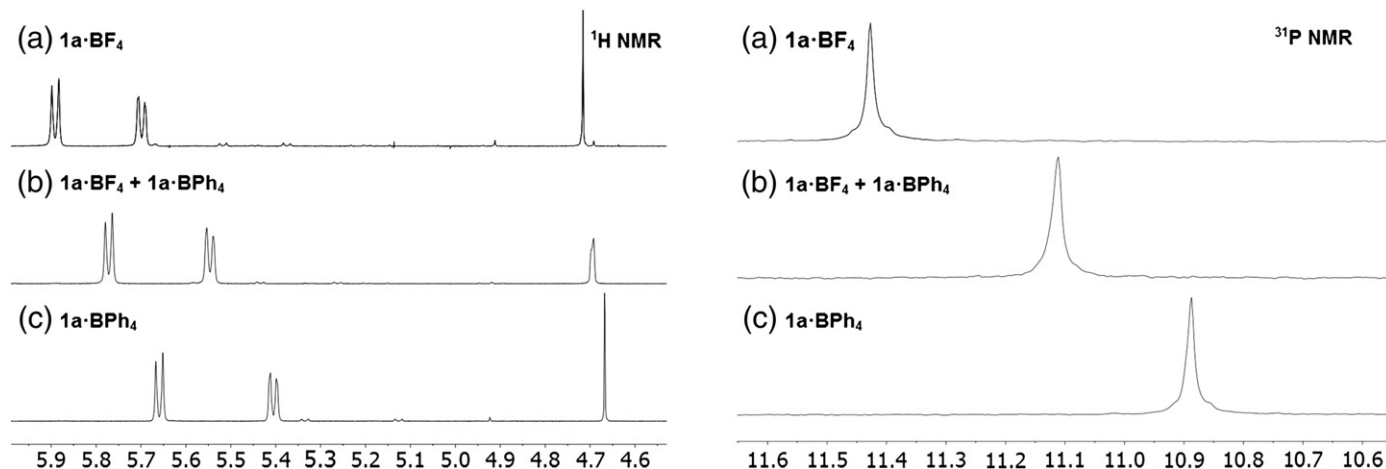


Fig. 2. (Left) Region of the aromatic *p*-cymene protons in the ^1H NMR spectra of (a) $1\mathbf{a}\cdot\text{BF}_4$, (b) an equimolar mixture of $1\mathbf{a}\cdot\text{BF}_4$ and $1\mathbf{a}\cdot\text{BPh}_4$ and (c) $1\mathbf{a}\cdot\text{BPh}_4$. (Right) $^{31}\text{P}\{^1\text{H}\}$ NMR spectra of (a) $1\mathbf{a}\cdot\text{BF}_4$, (b) an equimolar mixture of $1\mathbf{a}\cdot\text{BF}_4$ and $1\mathbf{a}\cdot\text{BPh}_4$ and (c) $1\mathbf{a}\cdot\text{BPh}_4$. CDCl_3 was used as solvent in all the experiments.

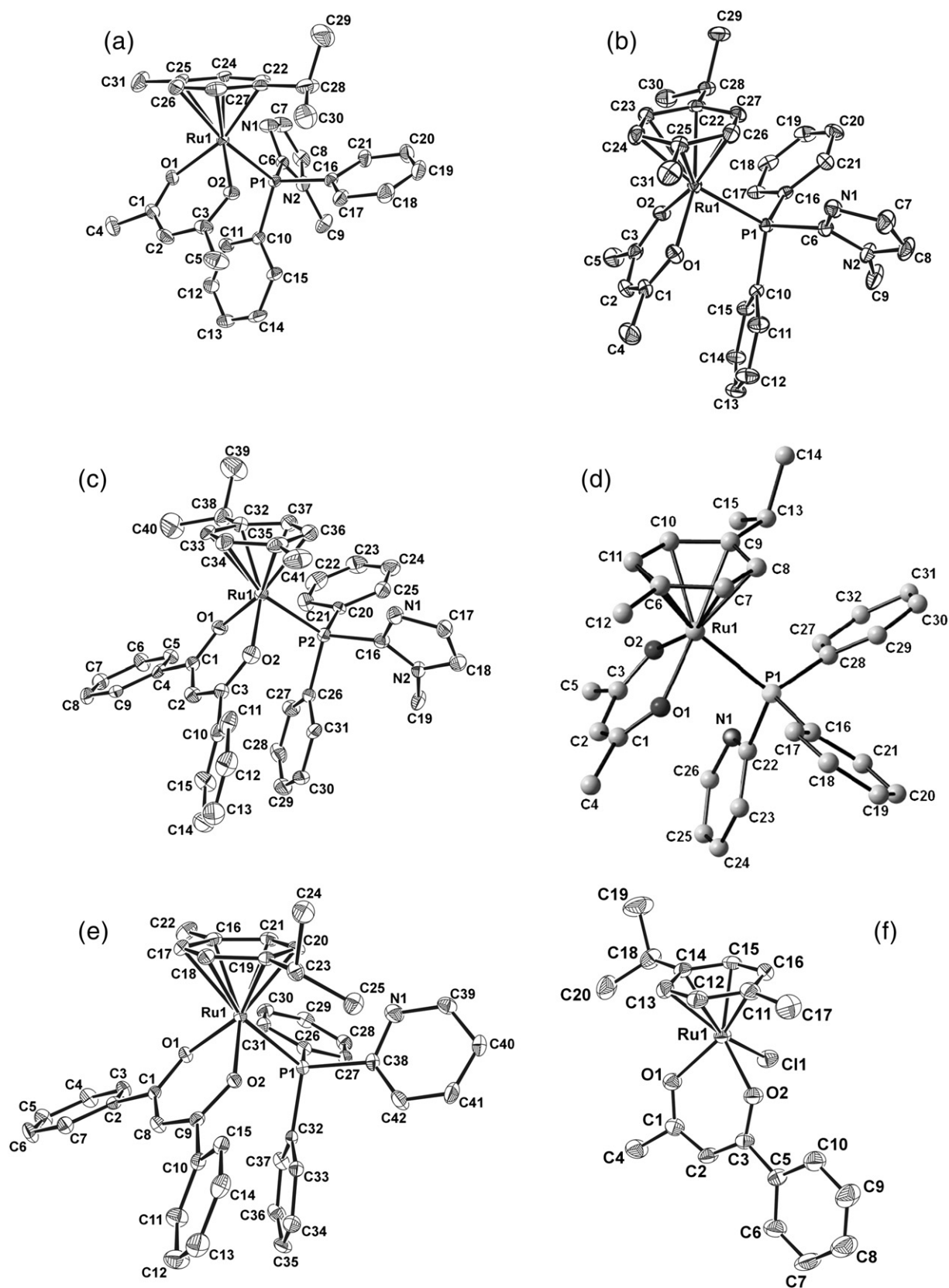


Fig. 3. ORTEP or ball and stick drawing of the complex cations: (a) $[(p\text{-cym})\text{Ru}(\text{acac})(\text{dpim})]\text{BF}_4$ (**1a**·**BF**₄), (b) $[(p\text{-cym})\text{Ru}(\text{acac})(\text{dpim})]\text{BPh}_4$ (**1a**·**BPh**₄), (c) $[(p\text{-cym})\text{Ru}(\text{dbzm})(\text{dpim})]\text{BF}_4$ (**3a**·**BF**₄), (d) $[(p\text{-cym})\text{Ru}(\text{acac})(\text{PPh}_2\text{Ppy})]\text{BPh}_4$ (**1b**·**BPh**₄), (e) $[(p\text{-cym})\text{Ru}(\text{dbzm})(\text{Ph}_2\text{Ppy})]\text{BPh}_4$ (**3b**·**BPh**₄), (f) **2**. Hydrogens and counterions have been omitted for clarity.

Table 2
Crystal data and structure refinement for **1a·BF₄**, **1a·BPh₄**, **1b·BPh₄**, **2**, **3a·BF₄** and **3b·BPh₄**.

	1a·BF ₄	1a·BPh ₄	1b·BPh ₄	2	3a·BF ₄	3b·BPh ₄
Empirical formula	C ₃₁ H ₃₆ BF ₄ N ₂ O ₂ PRu	C ₅₅ H ₅₆ BN ₂ O ₂ PRu	C ₅₆ H ₅₅ BNO ₂ PRu	C ₂₀ H ₂₃ ClO ₂ Ru	C ₄₁ H ₄₀ BF ₄ N ₂ O ₂ PRu	C ₆₆ H ₅₉ BNO ₂ PRu
Formula weight	687.47	919.87	916.86	431.90	811.60	1040.99
Temperature (K)	173(2)	173(2)	100(2)	298(2)	173(2)	100(2)
Wavelength (Å)	0.71073	0.71073	0.71073	0.71073	0.71073	0.71073
Crystal system	Monoclinic	Monoclinic	Monoclinic	Triclinic	Orthorhombic	Triclinic
Space group	C2/c	P2 ₁	P2 ₁ /n	P1	P2 ₁ 2 ₁ 2 ₁	P1
a(Å)	38.455(4)	10.260(2)	20.368(6)	9.6072(9)	10.043(2)	9.5301(3)
b(Å)	9.384(1)	21.274(3)	11.325(3)	12.138(1)	18.874(4)	15.9563(5)
c(Å)	18.523(2)	11.662(2)	20.480(5)	16.762(1)	19.405(4)	17.3447(6)
α(°)				92.881(2)		91.628(2)
β(°)	112.962(2)	113.09(2)	105.138(7)	103.513(2)		100.313(2)
γ(°)				96.531(2)		96.294(2)
Volume (Å ³)	6155(1)	2341.6(6)	4560(2)	1882.2(3)	3678(1)	2576.2(1)
Z	8	2	4	4	4	2
Density (calculated) (g/cm ³)	1.484	1.305	1.335	1.524	1.465	1.342
Absorption coefficient (mm ⁻¹)	0.617	0.412	0.423	0.983	0.529	0.383
F(000)	2816	960	1912	880	1664	1084
Crystal size (mm ³)	0.45 × 0.30 × 0.11	0.60 × 0.60 × 0.10	0.11 × 0.10 × 0.03	0.10 × 0.10 × 0.03	0.50 × 0.10 × 0.05	0.29 × 0.21 × 0.08
Index ranges	−45 ≤ h ≤ 45 −11 ≤ k ≤ 11 −22 ≤ l ≤ 22	−12 ≤ h ≤ 12 −25 ≤ k ≤ 25 −13 ≤ l ≤ 13	−20 ≤ h ≤ 19 −11 ≤ k ≤ 11 −16 ≤ l ≤ 20	−11 ≤ h ≤ 11 −14 ≤ k ≤ 14 −19 ≤ l ≤ 19	−11 ≤ h ≤ 11 −22 ≤ k ≤ 22 −23 ≤ l ≤ 23	−11 ≤ h ≤ 11 −19 ≤ k ≤ 19 0 ≤ l ≤ 21
Reflections collected	28995	23083	20851	18735	36333	10045
Independent reflections	5354 [R(int) = 0.1262]	8235 [R(int) = 0.1045]	4739 [R(int) = 0.2256]	6619 [R(int) = 0.0471]	6468 [R(int) = 0.1170]	10045 [R(int) = 0.0000]
Data/restraints/parameters	5354/0/417	8235/1/565	4739/0/259	6619/0/447	6468/0/470	10045/0/670
Goodness-of-fit on F ²	0.990	1.018	0.853	0.923	1.035	1.017
Final R indices [I > 2σ(I)]	R1 = 0.0640 wR2 = 0.1375	R1 = 0.0380 wR2 = 0.0772	R1 = 0.0752 wR2 = 0.1589	R1 = 0.0353 wR2 = 0.0732	R1 = 0.0872 wR2 = 0.2008	R1 = 0.0332 wR2 = 0.0697
Absolute structure parameter		−0.05(2)			−0.05(6)	
Largest diff. peak and hole	1.627 and −1.032	0.366 and −0.470	0.522 and −0.569	0.712 and −0.448	1.145 and −0.922	0.444 and −0.638

2.37 Å and this compares well with those of **A** [21] [2.352 Å] and **B** [49] [2.364 Å].

As stated, the β-diketonate groups adopt a bidentate coordination mode through the two O atoms to form a six-membered chelate ring. The O(2)–Ru(1)–O(1) bite angles are between 86.8° and 89.61° and this reveals the absence of strain. The Ru–O distances are quite similar for all the structures regardless of the nature of the β-diketonate (see Table 3). There is a difference between **1a·BF₄** and **1a·BPh₄**, suggesting that the counter-ion could affect the electronic distribution throughout the cationic complex. The C–O bond distances are slightly shorter for the acac complexes (about 1.27 Å with one value of 1.315 Å) as compared to the dbzm derivatives (about 1.29 Å), a situation in agreement with the higher electron-withdrawing ability of phenyl groups in comparison to the methyl groups and described for similar compounds [23]. In the case of **2**, which contains bzac (with a methyl and a phenyl group), the value found is intermediate (1.28 Å). The chelate rings are not completely planar and have an envelope conformation in all cases, with rather small dihedral angles between the diketonate backbone and the respective O–Ru–O planes (in the range 8.35–15.70°).

Unfortunately, interionic contacts cannot be accurately studied for the available structures of **1a·BF₄** and **3a·BF₄** because BF₄[−] anions show both positional and rotational disorder. Nevertheless, a rough analysis allowed us to confirm the presence of the BF₄[−] anions in the vicinity of the *p*-cymene flanks in the crystal network of both

complexes. This insinuates feasible C–H⋯F contacts between the BF₄[−] counterions and the *p*-cymene ring, a situation consistent with the NMR deshielding of the cymene signals.

In contrast to the above, the bigger BPh₄[−] anion does not show disorder in the crystal structures of **1a·BPh₄** and **3b·BPh₄**, and thus the interactions between the BPh₄[−] and the cationic complexes could be analyzed. In both cases, one or two BPh₄[−] anions seem to wrap the *p*-cymene ring of the Ru cation and at least one phenyl group establishes a CH–π interaction with an H atom of the coordinated *p*-cymene, as previously observed in related systems [55]. In fact, these contacts seem to be strong enough to remain in chloroform-*d*₆ solutions and they shield the aromatic protons of *p*-cymene (see NMR discussion). This CH–π interaction is depicted in Fig. 4 for derivative **1a·BPh₄** and the corresponding parameters for these anion-cation interactions for **1a·BPh₄** and **3b·BPh₄** are summarized in Table 4 and represented in Fig. S1 [56–58].

Similar complexes of formula [(η⁶-*p*-cymene)Ru(β-diketonate)(PTA)]BPh₄ (**D** type in Scheme 1) also show weak π interactions between the *p*-cymene entity and two different BPh₄[−] anions, as deduced by the Mercury program. In this case, each anion uses two phenyl groups to wrap both sides of the coordinated arene. Diversely, the corresponding BF₄[−] complexes, [(η⁶-*p*-cymene)Ru(β-diketonate)(PTA)]BF₄, show hydrogen bonds between the *p*-cymene ring and the BF₄[−] anions [23].

Table 3
Selected bond lengths [Å] and angles (°) for **1a·BF₄**, **1a·BPh₄**, **3a·BF₄**, **1b·BPh₄**, **3b·BPh₄** and **2**.

Bond length/angle	1a·BF ₄	1a·BPh ₄	1b·BPh ₄	3a·BF ₄	3b·BPh ₄	Bond length/angle	2
Ru-arene (centroid)	1.693	1.691	1.693	1.711	1.702	Ru-arene (centroid)	1.655
Ru(1)–P(1)	2.358(1)	2.341(1)	2.352(3)	2.352(2)	2.377(6)	Ru(1)–Cl(1)	2.410(1)
Ru(1)–O(1)	2.074(2)	2.061(3)	2.053(7)	2.080(6)	2.063(1)	Ru(1)–O(1)	2.079(3)
Ru(1)–O(2)	2.073(2)	2.070(2)	2.075(8)	2.076(6)	2.062(1)	Ru(1)–O(2)	2.074(3)
O(1)–Ru(1)–O(2)	87.9(1)	88.4(1)	89.7(3)	88.4(2)	88.51(6)	O(1)–Ru(1)–O(2)	86.8(1)
O(1)–Ru(1)–P(1)	89.31(8)	89.2(1)	84.2(2)	84.7(2)	84.78(4)	O(1)–Ru(1)–Cl(1)	84.84(9)
O(2)–Ru(1)–P(1)	83.29(8)	83.8(1)	88.7(2)	88.2(2)	88.03(4)	O(2)–Ru(1)–Cl(1)	85.02(9)

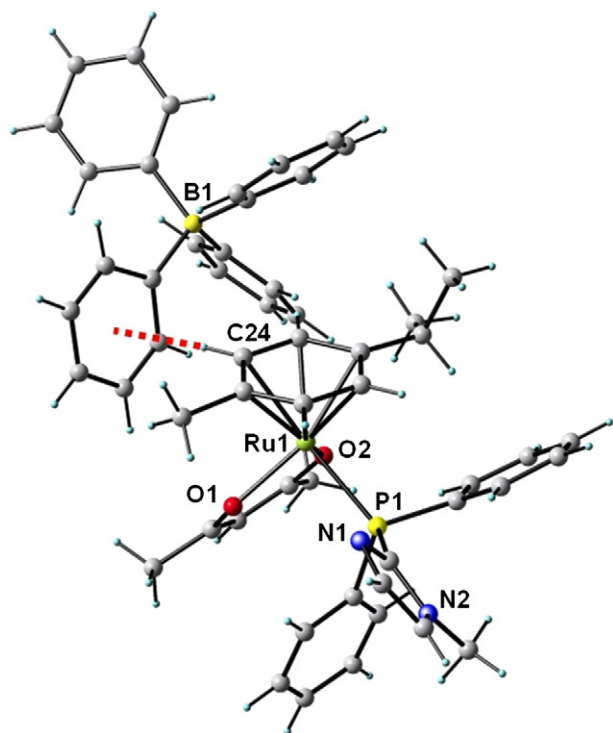


Fig. 4. CH- π interaction in complex **1a·BPh₄**, where *p*-cym is the C–H donor and B-Ph the acceptor ring.

3.3. Calculations of electrostatic potential surfaces and optimization of ionic pairs

Electrostatic potential maps were obtained for the complex cation **1a⁺** and for anions **BF₄⁻** and **BPh₄⁻** (Fig. 5) through DFT energy calculations in order to visualize charge distributions and locate the probable areas involved in electrostatic supramolecular (interionic) interactions. Calculations were performed using experimental structural parameters for **1a⁺** in **1a·BF₄**, whereas the structures of both anions were optimized in gas phase. Major positive charge regions were found on the hydrogen atoms of the *p*-cymene ring. On the other hand, the **BPh₄⁻** diagram shows that the negative charge is located on the π -electronic cloud of the electron-rich aromatic rings, while the hydrogens of the Ph groups have less electron density. Thus, it seems reasonable to find this anion involved in noncovalent CH- π interactions with the Ru-cymene cationic fragment, which acts as the hydrogen donor. As a matter of fact, a recent study emphasized the enhanced CH- π donor ability of Ru-coordinated arenes on the basis of DFT calculations [59]. The **BF₄⁻** map, as expected, reveals that the F atoms are highly electronegative and are consequently prone to form hydrogen bonds. Hence, specific CH-F-**BF₃⁻** interactions with the *p*-cymene electropositive protons seem credible. Similar noncovalent contacts have been found for other Ru arene complexes with the same anions [55,60]. These predictions are in good agreement with the contacts observed in the crystal structures of **1a·BF₄**

Table 4

Parameters for the CH- π interactions in **1a·BPh₄** and **3b·BPh₄**, where *p*-cym is the C–H donor and B-Ph the acceptor ring (see Fig. S1 in Supporting Information).

Compound	d_{C-Ct} (Å)	d_{H-Ct} (Å)	d_{H-Atm} (Å)	α (°)
1a·BPh₄	3.57	2.64	2.87	163.95
3b·BPh₄	3.50	2.61	2.80	160.70

d_{C-Ct} = distance between the C atom in the C–H donor and the centroid of the acceptor ring; d_{H-Ct} = distance between the H atom in the C–H donor and the centroid of the acceptor ring; d_{H-Atm} = distance between the H atom in the C–H donor and the closest C atom in the acceptor ring; α = C–H-centroid angle (see Fig. S1).

and **1a·BPh₄** as well as with the evidence of ion-pairing observed in solution by ¹H NMR spectroscopy.

Theoretical studies were carried out in order to provide more information concerning the ion pairing nature in non-polar solvents. Initially, gas phase geometrical optimization of the ion pairs [(η^6 -*p*-cymene)Ru(acac)(dpim)]BF₄ (**1a·BF₄**) [(η^6 -*p*-cymene)Ru(acac)(dpim)]BPh₄ (**1a·BPh₄**) was carried out at the B3LYP level (see Computational studies section). The relative anion-cation orientations are very similar to the ones found in the solid state. In particular, in **1a·BF₄** there is a distance of 1.947 Å between a fluorine atom of the BF₄⁻ anion and a hydrogen atom of the *p*-cymene located in the *ortho* position to the ¹Pr substituent, with a C(H)⋯F distance of 3.028 Å and a C–H⋯F angle of 173.16°. These values are consistent with a strong hydrogen bonding interaction [61]. There is also a short distance between a fluorine atom of the anion and a hydrogen atom of a methyl group of the coordinated acetylacetonate (2.036 Å). In this case, the C(H)⋯F distance is 3.120 Å and the C–H⋯F angle is 167.73°. These values account for another hydrogen bond.

In **1a·BPh₄** there is a distance of 2.604 Å between a hydrogen atom of the *p*-cymene and the centroid of a phenyl ring of the anion BPh₄⁻. In addition, the shortest H(*p*-cymene)⋯C(phenyl) distance is 2.714 Å and the C–H-centroid angle is 177.43°. These values fit well with the reference parameters for a CH- π interaction [62,63].

In an effort to explain the formation of the ionic pairs in solution with solvents of low polarity, free energies of solvation were calculated for **1a·BF₄** and **1a·BPh₄** in chloroform and water (see Computational studies section). The stabilization of the ionic pairs with respect to the gas phase is higher for chloroform than for water. In the case of **1a·BF₄** the difference is 6.2 kcal/mol in favor of chloroform and in the case of **1a·BPh₄** this difference is 10.3 kcal/mol, again in favor of chloroform. All in all, these results support the stabilization of the ionic pairs **1a·BF₄** and **1a·BPh₄** in solution when solvents of low polarity are used, a situation in good agreement with the aforementioned NMR evidence, i.e. the differences in the chemical shifts for the two different salts.

In addition, NBO [64] calculations were performed in order to determine the charges on the phosphorus atom in the ion pairs **1a·BF₄** and **1a·BPh₄**. The calculated charges are 1.055 for **1a·BF₄** and 1.054 for **1a·BPh₄**. As can be seen, the charge on the phosphorus atom for **1a·BF₄** is slightly more positive than the charge for the same atom in **1a·BPh₄**. This is in accordance with the observed differences in the ³¹P NMR resonances, since the more positive phosphorus in **1a·BF₄** appears at higher frequencies (less shielded) and the less positive phosphorus atom (in **1a·BPh₄**) appears at lower frequencies. This confirms that the donation of electron density from the P to the Ru ion is slightly lower in **1a·BPh₄** as a consequence of the interaction between the counter-ion and the arene, which would affect the electronic distribution throughout the complex.

3.4. DNA-ruthenium complex interaction studies

DNA is the main biological target for most of the anticancer compounds. In order to evaluate the ability of our ruthenium complexes to bind to DNA, agarose gel electrophoresis and atomic force microscopy studies were carried out. For comparison purposes, cisplatin was considered as the reference drug and it was also evaluated under the same experimental conditions.

Complex **1b·BF₄** was excluded from these experiments because it is very unstable and the BPh₄ derivatives were also discarded because they were insoluble in water. The same applies for the cytotoxicity studies.

3.4.1. Agarose gel electrophoresis

The influence of the compounds on the tertiary structure of DNA was determined by their ability to modify the electrophoretic mobility of the relaxed open circular form (OC) and/or supercoiled

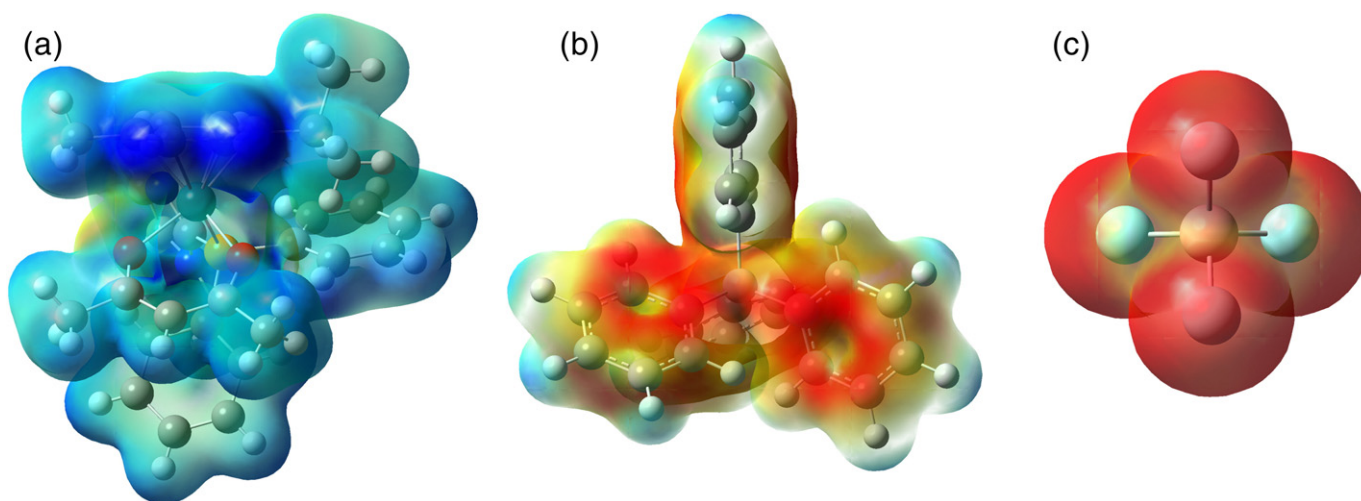


Fig. 5. Electrostatic potential maps for: the complex cation $1a^+$ (a), and anions BPh_4^- (b) and BF_4^- (c). The most electronegative areas are in red and the least electronegative areas in blue.

covalently closed circular form (CCC) of the pBR322 plasmid DNA. The electrophoretic mobility of these two forms is very different since it depends on the degree of DNA folding. The BF_4 complexes $1a \cdot BF_4$, $2a \cdot BF_4$, $3a \cdot BF_4$, $2b \cdot BF_4$ and $3b \cdot BF_4$ were tested after 48 h of incubation with the plasmid DNA at the molar ratio $r_i = 0.50$. As shown in Fig. 6, complexes $1a \cdot BF_4$, $2a \cdot BF_4$ and $3a \cdot BF_4$ (lanes 5, 6, and 7) did not give rise to observable interactions with the DNA as the degree of folding of the OC and/or CCC forms of the plasmid was unaltered by the presence of the ruthenium complexes. In sharp contrast, under similar conditions, cisplatin and complexes $2b \cdot BF_4$ and $3b \cdot BF_4$ induced significant changes in the electrophoretic mobility of these plasmid forms. While cisplatin induced a co-migration of the two DNA bands, next to the coalescence point (lanes 3 and 4) [65], compounds $2b \cdot BF_4$ (lane 8) and $3b \cdot BF_4$ (lane 9) produced an appreciable progressive conversion of the CCC bands into the OC bands, indicating that the supercoiled plasmid DNA forms were relaxed by the interaction with the ruthenium complexes. Similar results were obtained when the incubation time of the samples was reduced to 24 h (see Fig. S3 in Supplementary material).

3.4.2. AFM studies

Tapping mode atomic force microscopy (TMAFM) is an excellent tool to study the surface relief, morphology and topology of DNA molecules [66,67]. With this technique, direct visualization of three conformers of pBR322 plasmid DNA can be achieved and therefore

modifications caused in these conformers, after being incubated in the presence of the ruthenium compounds, can be graphically evaluated. Based on the DNA-interacting behavior observed in the electrophoretic mobility experiments, complexes $2b \cdot BF_4$ and $3b \cdot BF_4$ were selected for further analysis by AFM. The AFM images in Fig. 7 are of free pBR322 plasmid DNA without any treatment (A), pBR322 incubated for 48 h at 37 °C ($r_i = 0.5$) with cisplatin as positive control (B), and with BF_4 complexes $2b \cdot BF_4$ and $3b \cdot BF_4$ (C and D, respectively). The typical AFM image of native pBR322 can be observed in Fig. 7A. In Fig. 7B it can be seen that DNA structure is distorted by cisplatin through the development of numerous kinks in the DNA chains, which is very characteristic of this compound as it covalently binds to DNA. In addition, the ability of cisplatin to crosslink DNA led to the formation of some plasmid aggregates [66,68,69], a situation in accordance with the significant decrease in electrophoretic mobility of the conformer forms. It can be seen in Fig. 7C and D that the interaction of both $2b \cdot BF_4$ and $3b \cdot BF_4$ with DNA produced similar changes in structure, with a general tendency to induce relaxed circular forms and some cross-links between plasmids. However, a reduced number of kinked forms were present in the DNA chains compared with cisplatin-treated samples. The conformational changes in the plasmid DNA structure induced by these compounds may presumably be attributed to covalent interactions between ruthenium and DNA. These interactions are similar to those induced by cisplatin or cisplatin(II) analogues [70–73] and very different

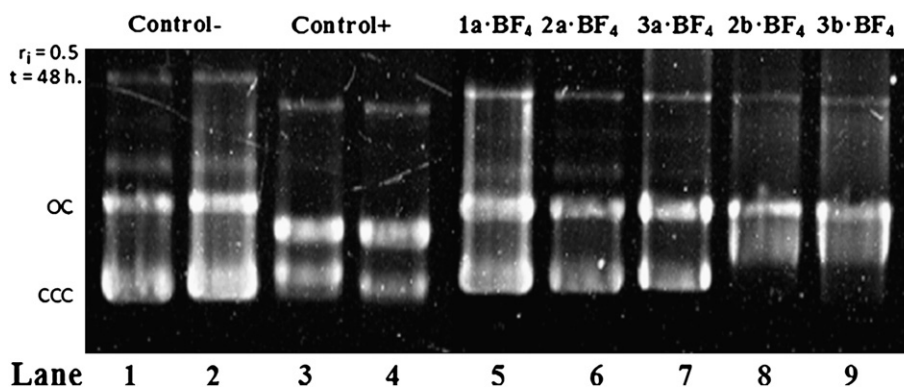


Fig. 6. Electrophoretic mobility pattern in agarose gel of pBR322 plasmid DNA treated with $1a \cdot BF_4$ (lane 5), $2a \cdot BF_4$ (lane 6), $3a \cdot BF_4$ (lane 7), $2b \cdot BF_4$ (lane 8) and $3b \cdot BF_4$ (lane 9) for 48 h at 37 °C ($r_i = 0.5$). Control plasmid DNA samples treated with TE buffer and TE buffer + vehicle (milliQ water + 5% DMSO) are represented in lanes 1 and 2, respectively. Lanes 3 and 4 show the mobility pattern of the plasmid DNA incubated with cisplatin (dissolved in milliQ water alone and milliQ water + 5% DMSO). OC, open circular form; CCC, covalently closed circular form.

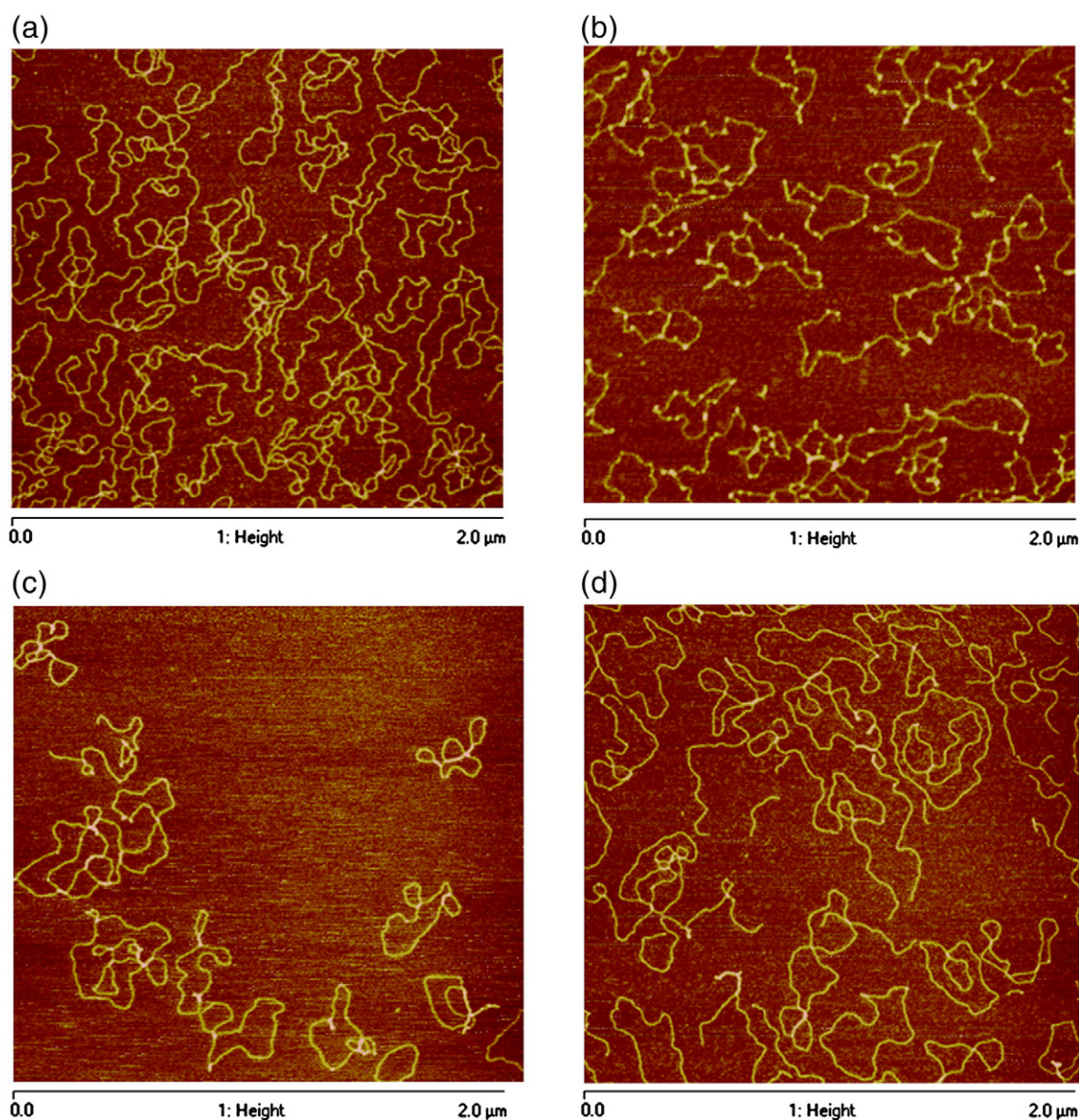


Fig. 7. AFM images of pBR322 plasmid DNA free (A) and incubated with cisplatin (B), $2b \cdot BF_4$ (C) and $3b \cdot BF_4$ (D) for 48 h at 37 °C ($r_i = 0.5$).

to those observed for classical intercalators such as ethidium bromide and other planar heterocycles [74,75]. Finally, it is important to highlight that both compounds were able to produce some fragmentation of DNA chains during the reaction, even in the absence of an activator. In conclusion, AFM results confirm that the new complexes $2b \cdot BF_4$ and $3b \cdot BF_4$ interact with DNA and modify its tertiary structure, as we previously observed in the electrophoretic pattern.

3.5. Cytotoxicity

The cytotoxic activity levels of the BF_4^- salts $1a \cdot BF_4$, $2a \cdot BF_4$, $3a \cdot BF_4$, $2b \cdot BF_4$ and $3b \cdot BF_4$ were established in a comparative *in vitro* MTT cell viability assay with both human breast cancer cells (MCF-7) and human pancreatic cancer cells (CAPAN-1). The different ruthenium compounds were freshly dissolved in DMSO and milli-Q water and then serially diluted in complete culture medium at concentrations ranging from 0 μM to 100 μM (DMSO final concentration in the culture medium <1%). The activity values are expressed as the concentration of each complex required to decrease the cell viability by 50% (IC_{50}). The five complexes displayed IC_{50} values below 50 μM in both MCF-7 (except complex $1a \cdot BF_4$) and CAPAN-1 cancer

cell lines (Table 5). Remarkably, complexes $2b \cdot BF_4$ and $3b \cdot BF_4$ were the most efficient at inhibiting the cell proliferation, with IC_{50} values equivalent to those established for cisplatin in these cell lines ($IC_{50} = 4 \mu M$ in MCF-7 cells and 2.5 μM in CAPAN-1 cells). The significant antiproliferative activity of these two complexes may be closely related to their ability to interact with DNA. However, we cannot rule out other biological targets for these complexes, most likely proteins, as complexes $1a \cdot BF_4$, $2a \cdot BF_4$ and $3a \cdot BF_4$, which did not interact with DNA in the *in vitro* experiments, have demonstrated relevant cytotoxic activity. On the other hand, the low solubility of these derivatives in water could limit their potential *in vivo* antitumor activity. Nevertheless, strategies such as the use of polymeric micelles as carrier systems for water-insoluble anticancer drugs could be helpful to improve the *in vivo* activity [76].

3.6. Stability studies

In order to obtain more information concerning the reasons for the different behavior of the dpim or PPh₂py Ru complexes in the interaction with DNA or in the cytotoxicity experiments, complementary studies on the stability of the Ru derivatives in the solvent mixture used for

Table 5
IC₅₀ (μM) values for the compounds **1a**·BF₄, **2a**·BF₄, **3a**·BF₄, **2b**·BF₄ and **3b**·BF₄.

Compound	MCF-7	CAPAN-1
1a ·BF ₄	62	23.67
2a ·BF ₄	19.67	35.33
3a ·BF ₄	22.95	25.5
2b ·BF ₄	3.77	6.6
3b ·BF ₄	3.3	6.94
Cisplatin	4	2.5

the AFM studies (DMSO/H₂O) and cyclic voltammetry of the new derivatives were undertaken.

Hydrolysis processes are of great interest to gain a more precise outlook about the stability of the potential drugs under pseudo-pharmacological conditions. However, all of our complexes are insoluble in water, so we monitored complexes **3a**·BF₄ and **3b**·BF₄ by ³¹P {¹H} NMR spectroscopy in a mixture of DMSO-d₆/D₂O (50:50) for several days. The dpim complex, **3a**·BF₄, showed high stability, since evolution was not observed after 48 h and only traces of evolution products were detected after 4 days (Fig. 8). By contrast, the PPh₂py derivative, **3b**·BF₄, displayed signs of hydrolytic evolution after 1 h and several emerging peaks were confirmed over the next 7 days (Fig. 9).

3.7. Cyclic voltammetry experiments

Cyclic voltammetry experiments were carried out on all the BF₄ salts – except for the unstable **1b**·BF₄ – in order to determine their redox behavior. The measurements were made on solutions of the respective complexes (10^{−3} M) and tetrabutylammonium hexafluorophosphate (TBAPF₆, 0.1 M) as the supporting salt, in dry CH₂Cl₂, using a conventional three-electrode cell with a graphite working electrode. In particular, the abovementioned BF₄ salts showed a Ru-based one-electron quasi-reversible oxidation (Ru^{III}/Ru^{II}) with E_{1/2} values between +0.82 and +0.76 V for complexes of series a, and +0.58 and +0.57 V for complexes of series b, with respect to a calomel reference electrode at a scan rate 100 mV·s^{−1} (see Table 6 and Fig. S2). The higher oxidation potentials observed for series a relative to series b suggest that dpim has a worse σ-donor character and/or a better π-acceptor character than PPh₂py, so that the Ru(II) ion becomes poorer in electron density in complexes of series a compared to their analogues in series b. As a consequence, the β-diketonate dissociation in water and subsequent

aquation would be enhanced for complexes belonging to series b. This finding is in agreement with the higher hydrolysis rate observed for **3b**·BF₄ relative to that of **3a**·BF₄ and can explain the different antiproliferative activities of the two series.

3.8. Pro-apoptotic activity studies

To further characterize the cytotoxicity of the BF₄ complexes, their pro-apoptotic activity was also determined. The disruption of the regulation of apoptosis is a key event in the transformation of normal cells into tumor cells and many traditional anticancer drugs exert their cytotoxic effects by inducing apoptosis, most often as a result of DNA damage [77,78]. Thus, it is important to evaluate the suitability of the complexes as possible anticancer agents in terms of their ability to induce apoptosis, as the cellular viability assays, like the MTT test, measure cytotoxicity but do not distinguish between apoptosis and necrosis. The pro-apoptotic activity of the complexes was quantified by annexin V–propidium iodide flow cytometry after treating CAPAN-1 cells for 24 h with two different concentrations (10 and 20 mM) of complex **2b**·BF₄, which demonstrated a high cytotoxic activity, or medium alone as a control. Annexin V binds phosphatidyl serine residues, which are asymmetrically distributed towards the inner plasma membrane but migrate to the outer plasma membrane during apoptosis. Propidium iodide is impermeant to live cells and apoptotic cells but stains nucleic acids in dead cells. Hence, the percentage of annexin V positive cells indicates the proportion of apoptotic cells, while double positive staining for annexin V and propidium iodide indicates both late apoptotic and necrotic cells (dead cells). As represented in Table 7, both **2b**·BF₄ concentrations markedly increased the percentage of apoptotic cells compared to the basal level of apoptosis seen in the control cells. The treatments also led to a relevant percentage of dead cells, which may be the result of either late apoptotic or necrotic pathways, as apoptosis develops rapidly after the treatment.

These results demonstrate that, according to their ability to interact with DNA, the complex induces cell death largely through the activation of apoptotic pathways.

4. Concluding remarks

A collection of new Ru(II) compounds of general formula [(η⁶-p-cymene)Ru(κ²-O,O'-X)(κ¹-P-L)]Y has been prepared through

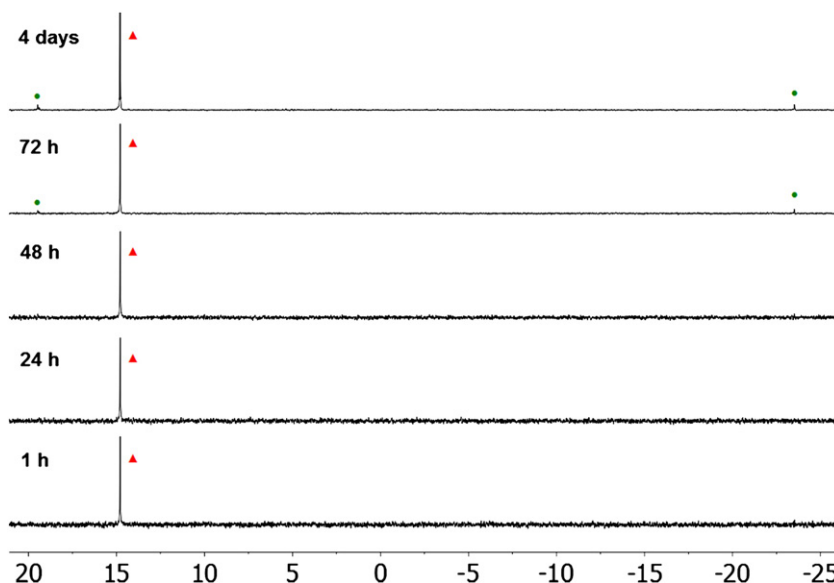


Fig. 8. Evolution with time of the ³¹P{¹H} NMR spectrum for **3a**·BF₄ (filled red triangle) in a mixture of DMSO-d₆/D₂O (50:50). Evolution products are labelled as (filled green circle).

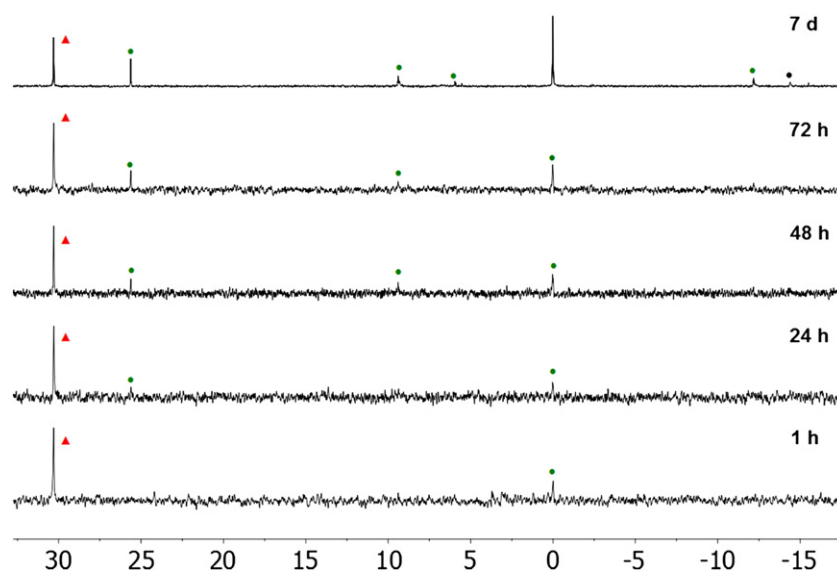


Fig. 9. Evolution with time of the $^{31}\text{P}\{^1\text{H}\}$ NMR spectrum for $3\mathbf{b}\cdot\text{BF}_4$ (filled red triangle) in a mixture of DMSO- d_6 /D $_2$ O (50:50). Evolution products are labelled as (filled green circle).

the combination of two aminophosphines ($L = \text{dpim}$ and PPh_2py) as neutral ligands, three β -diketonates ($X = \text{acac}$, bzac and dbzm) as monoanionic leaving groups, and two borate anions ($Y = \text{BF}_4^-$ and BPh_4^-) as counter-ions. NMR, structural and computational studies provide evidence of ion-pairing for these complexes with both BF_4^- and BPh_4^- in CDCl_3 . For the BF_4^- salts the ion-pairs are likely to be held together by interionic F–H–C hydrogen bonds, whereas for the BPh_4^- salts, CH– π interactions are thought to be the driving force for the ion pair formation. In addition, most of the complexes show a general tendency to lose the *p*-cymene ring slowly in apolar solvents such as CDCl_3 . On the other hand, the more soluble BF_4^- salts have shown cytotoxic activity in MTT assays with human breast cancer cells (MCF-7) and human pancreatic cancer cells (CAPAN-1). Interestingly, the most active complexes in both cell lines are those with PPh_2py , namely $2\mathbf{b}\cdot\text{BF}_4$ and $3\mathbf{b}\cdot\text{BF}_4$, which also exhibit a remarkable interaction with DNA – as established by electrophoretic and AFM studies. The corresponding analogs with dpim , $1\mathbf{a}\cdot\text{BF}_4$, $2\mathbf{a}\cdot\text{BF}_4$ and $3\mathbf{a}\cdot\text{BF}_4$, are less active and are reluctant to take part in any interaction with DNA. Moreover, evolution experiments suggest a correlation between these trends and the hydrolysis rate in DMSO/H $_2$ O solutions, so that the higher reactivity of $3\mathbf{b}\cdot\text{BF}_4$ as compared to $3\mathbf{a}\cdot\text{BF}_4$ could explain the enhanced biological performance of the former. This ligand effect is rationalized in terms of the electronic features of the two phosphines, as established by cyclic voltammetry measurements. In

Table 6
Cyclic voltammetric data for BF_4 salts of series a and b.

Compound	E_{ox} (V)	E_{red} (V)	$E_{1/2}$ (V)
$1\mathbf{a}\cdot\text{BF}_4$	0.8	0.71	0.76
$2\mathbf{a}\cdot\text{BF}_4$	0.34	0.27	0.31
	0.83	0.77	0.80
$3\mathbf{a}\cdot\text{BF}_4$	0.85	0.79	0.82
$2\mathbf{b}\cdot\text{BF}_4$	0.59	0.54	0.565
$3\mathbf{b}\cdot\text{BF}_4$	0.62	0.54	0.58

Table 7
Percentage of live, apoptotic and dead cells after treating CAPAN-1 cells with the complex $2\mathbf{b}\cdot\text{BF}_4$ for 24 h.

Compound	% Live	% Apoptotic	% Dead
Blank	87.7%	5.8%	5.9%
$2\mathbf{b}\cdot\text{BF}_4$ 10 μM	62.6%	21.0%	15.8%
$2\mathbf{b}\cdot\text{BF}_4$ 20 μM	56.5%	19.8%	22.0%

summary, we are inclined to believe that activation by β -diketonate dissociation and aquation might be favored in complexes that belong to series b due to the higher σ -donor ability of PPh_2py compared to dpim . In addition, we believe that two attributes of our complexes contribute to their cytotoxic properties by avoiding premature reactions on the metallic center: (i) the strong binding of the β -diketonate anions to the Ru(II) ion as compared with other monodentate ligands such as chloro [79,80] and (ii) protection of the metal by the pendant groups in the arene entity and the bulky substituents on the β -diketonate ligands [24].

Acknowledgments

This work was supported by the MINECO of Spain (project CTQ-2011-24434, FEDER funds). We would like to acknowledge Emilie Goossens for technical support.

Appendix A. Supplementary data

Supplementary data to this article can be found online at <http://dx.doi.org/10.1016/j.jinorgbio.2012.07.022>.

References

- [1] G. Süß-Fink, Dalton Trans. 39 (2010) 1673–1688.
- [2] Y.K. Yan, M. Melchart, A. Habtemariam, P.J. Sadler, Chem. Commun. (2005) 4764–4776.
- [3] H.M. Chen, J.A. Parkinson, S. Parsons, R.A. Coxall, R.O. Gould, P.J. Sadler, J. Am. Chem. Soc. 124 (2002) 3064–3082.
- [4] R.E. Morris, R.E. Aird, P.D. Murdoch, H.M. Chen, J. Cummings, N.D. Hughes, S. Parsons, A. Parkin, G. Boyd, D.I. Jodrell, P.J. Sadler, J. Med. Chem. 44 (2001) 3616–3621.
- [5] B. Wu, M.S. Ong, M. Groessl, Z. Adhikarsan, C.G. Hartinger, P.J. Dyson, C.A. Davey, Chem.-Eur. J. 17 (2011) 3562–3566.
- [6] C. Scolaro, A. Bergamo, L. Brescacin, R. Delfino, M. Cocchietto, G. Laurenczy, T.J. Geldbach, G. Sava, P.J. Dyson, J. Med. Chem. 48 (2005) 4161–4171.
- [7] R.E. Aird, J. Cummings, A.A. Ritchie, M. Muir, R.E. Morris, H. Chen, P.J. Sadler, D.I. Jodrell, Br. J. Cancer 86 (2002) 1652–1657.
- [8] S.H. van Rijt, P.J. Sadler, Drug Discov. Today 14 (2009) 1089–1097.
- [9] W.H. Ang, A. Casini, G. Sava, P.J. Dyson, J. Organomet. Chem. 696 (2011) 989–998.
- [10] G. Sava, A. Bergamo, P.J. Dyson, Dalton Trans. 40 (2011) 9069–9075.
- [11] W.H. Ang, P.J. Dyson, Eur. J. Inorg. Chem. (2006) 4003–4018.
- [12] G.S. Smith, B. Therrien, Dalton Trans. 40 (2011) 10793–10800.
- [13] A. Bergamo, G. Sava, Dalton Trans. 40 (2011) 7817–7823.
- [14] E. Meggers, G.E. Atilla-Gokcumen, K. Grundler, C. Frias, A. Prokop, Dalton Trans. (2009) 10882–10888.
- [15] C.A. Vock, W.H. Ang, C. Scolaro, A.D. Phillips, L. Lagopoulos, L. Juillerat-Jeanerret, G. Sava, R. Scopelliti, P.J. Dyson, J. Med. Chem. 50 (2007) 2166–2175.
- [16] M.G. Mendoza-Ferri, C.G. Hartinger, R.E. Eichinger, N. Stolyarova, K. Severin, M.A. Jakupec, A.A. Nazarov, B.K. Keppler, Organometallics 27 (2008) 2405–2407.

- [17] M. Cunningham, A. McCrate, M. Nielsen, S. Swavey, *Eur. J. Inorg. Chem.* (2009) 1521–1525.
- [18] S. Rani-Beeram, K. Meyer, A. McCrate, Y.L. Hong, M. Nielsen, S. Swavey, *Inorg. Chem.* 47 (2008) 11278–11283.
- [19] S.J. Dougan, A. Habtemariam, S.E. McHale, S. Parsons, P.J. Sadler, *Proc. Natl. Acad. Sci. U. S. A.* 105 (2008) 11628–11633.
- [20] P. Espinet, K. Soulantica, *Coord. Chem. Rev.* 193–5 (1999) 499–556.
- [21] A. Caballero, F.A. Jalon, B.R. Manzano, G. Espino, M. Perez-Manrique, A. Mucientes, F.J. Pobleto, M. Maestro, *Organometallics* 23 (2004) 5694–5706.
- [22] P. Nowak-Sliwinska, J.R. van Beijnum, A. Casini, A.A. Nazarov, G. Wagnieres, H. van den Bergh, P.J. Dyson, A.W. Griffioen, *J. Med. Chem.* 54 (2011) 3895–3902.
- [23] C.A. Vock, A.K. Renfrew, R. Scopelliti, L. Juillerat-Jeanneret, P.J. Dyson, *Eur. J. Inorg. Chem.* (2008) 1661–1671.
- [24] A. Habtemariam, M. Melchart, R. Fernandez, S. Parsons, I.D.H. Oswald, A. Parkin, F.P.A. Fabbiani, J.E. Davidson, A. Dawson, R.E. Aird, D.I. Jodrell, P.J. Sadler, *J. Med. Chem.* 49 (2006) 6858–6868.
- [25] R.A. Zelonka, M.C. Baird, *Can. J. Chem.* 50 (1972) 3063–3072.
- [26] M.A. Bennett, A.K. Smith, *J. Chem. Soc.-Dalton Trans.* (1974) 233–241.
- [27] M.A. Jalil, T. Yamada, S. Fujinami, T. Honjo, H. Nishikawa, *Polyhedron* 20 (2001) 627–633.
- [28] S.L. Nongbri, B. Das, K.M. Rao, *J. Organomet. Chem.* 694 (2009) 3881–3891.
- [29] K.S. Singh, K.A. Kreisel, G.P.A. Yap, M.R. Kollipara, *J. Organomet. Chem.* 691 (2006) 3509–3518.
- [30] G.R. Fulmer, A.J.M. Miller, N.H. Sherden, H.E. Gottlieb, A. Nudelman, B.M. Stoltz, J.E. Bercaw, K.I. Goldberg, *Organometallics* 29 (2011) 2176–2179.
- [31] SAINT+ v7.12a, Area-Detector Integration Program, Bruker-Nonius AXS, Madison, Wisconsin, USA, 2004.
- [32] G.M. Sheldrick, SADABS version 2004/1. A Program for Empirical Absorption Correction, University of Göttingen, Göttingen, Germany, 2004.
- [33] SHELXTL-NT version 6.12, Structure Determination Package, Bruker-Nonius AXS, Madison, Wisconsin, USA, 2001.
- [34] M.J. Frisch, G.W. Trucks, H.B. Schlegel, G.E. Scuseria, M.A. Robb, J.R. Cheeseman, J. Montgomery, J. A., T. Vreven, K.N. Kudin, J.C. Burant, J.M. Millam, S.S. yengar, J. Tomasi, V. Barone, B. Mennucci, M. Cossi, G. Scalmani, N. Rega, G.A. Petersson, H. Nakatsuji, M. Hada, M. Ehara, K. Toyota, R. Fukuda, J. Hasegawa, M. Ishida, T. Nakajima, Y. Honda, O. Kitao, H. Nakai, M. Klene, X. Li, J.E. Knox, H.P. Hratchian, J.B. Cross, C. Adamo, J. Jaramillo, R. Gomperts, R.E. Stratmann, O. Yazyev, A.J. Austin, R. Cammi, C. Pomelli, J.W. Ochterski, P.Y. Ayala, K. Morokuma, G.A. Voth, P. Salvador, J.J. Dannenberg, V.G. Zakrzewski, S. Dapprich, A.D. Daniels, M.C. Strain, O. Farkas, D.K. Malick, A.D. Rabuck, K. Raghavachari, J.B. Foresman, J.V. Ortiz, Q. Cui, A.G. Baboul, S. Clifford, J. Cioslowski, B.B. Stefanov, G. Liu, A. Liashenko, P. Piskorz, I. Komaromi, R.L. Martin, D.J. Fox, T. Keith, M.A. Al-Laham, C.Y. Peng, A. Nanayakkara, M. Challacombe, P.M.W. Gill, B. Johnson, W. Chen, M.W. Wong, C. Gonzalez, J.A. Pople, GAUSSIAN 03, Revision C.02, Gaussian, Inc., Wallingford, CT, 2004.
- [35] A.D. Becke, *J. Chem. Phys.* 98 (1993) 5648–5652.
- [36] C.T. Lee, W.T. Yang, R.G. Parr, *Phys. Rev. B* 37 (1988) 785–789.
- [37] M.M. Francl, W.J. Pietro, W.J. Hehre, J.S. Binkley, M.S. Gordon, D.J. Defrees, J.A. Pople, *J. Chem. Phys.* 77 (1982) 3654–3665.
- [38] P.C. Hariharan, J.A. Pople, *Theor. Chim. Acta* 28 (1973) 213–222.
- [39] P.J. Hay, W.R. Wadt, *J. Chem. Phys.* 82 (1985) 299–310.
- [40] GaussView 4.1, Gauss, Inc., Wallingford, CT, 2006.
- [41] V. Barone, M. Cossi, *J. Phys. Chem. A* 102 (1998) 1995–2001.
- [42] M. Cossi, N. Rega, G. Scalmani, V. Barone, *J. Comput. Chem.* 24 (2003) 669–681.
- [43] M. Namazian, S. Halvani, M.R. Noorbala, *THEOCHEM J. Mol. Struct.* 711 (2004) 13–18.
- [44] R.F. Winter, F.M. Hornung, *Inorg. Chem.* 36 (1997) 6197–6204.
- [45] K. Nakamoto *Journal* (2009) Pages.
- [46] P. Govindaswamy, S.M. Mobin, C. Thone, M.R. Kollipara, *J. Organomet. Chem.* 690 (2005) 1218–1225.
- [47] W.J. Geary, *Coord. Chem. Rev.* 7 (1971) 81 &.
- [48] R. Lalrempuia, P.J. Carroll, M.R. Kollipara, *J. Chem. Sci.* 116 (2004) 21–27.
- [49] I. Moldes, E. de la Encarnación, J. Ros, A. Alvarez-Larena, J.F. Piniella, *J. Organomet. Chem.* 566 (1998) 165–174.
- [50] H. Friebolin, *J.K. Beccosall Journal* (1998) Pages.
- [51] C. Ganter, *Chem. Soc. Rev.* 32 (2003) 130–138.
- [52] A.B. Chaplin, P.J. Dyson, *J. Organomet. Chem.* 696 (2011) 2485–2490.
- [53] A.B. Chaplin, C. Fellay, G. Laurency, P.J. Dyson, *Organometallics* 26 (2007) 586–593.
- [54] C. Daguene, R. Scopelliti, P.J. Dyson, *Organometallics* 23 (2004) 4849–4857.
- [55] D. Zuccaccia, G. Bellachioma, G. Cardaci, G. Ciancaleoni, C. Zuccaccia, E. Clot, A. Macchioni, *Organometallics* 26 (2007) 3930–3946.
- [56] M. Nishio, *CrystEngComm* 6 (2004) 130–158.
- [57] G.A. Bogdanovic, A.S.D. Bire, S.D. Zaric, *Eur. J. Inorg. Chem.* (2002) 1599–1602.
- [58] S. Tsuzuki, A. Fujii, *Phys. Chem. Chem. Phys.* 10 (2008) 2584–2594.
- [59] S.T. Mutter, J.A. Platts, *J. Phys. Chem. A* 115 (2011) 11293–11302.
- [60] A. Moreno, P.S. Pregosin, G. Laurency, A.D. Phillips, P.J. Dyson, *Organometallics* 28 (2009) 6432–6441.
- [61] T. Steiner, *Angew. Chem. Int. Ed.* 41 (2002) 48–76.
- [62] S. Tsuzuki, K. Honda, T. Uchimaru, M. Mikami, K. Tanabe, *J. Am. Chem. Soc.* 122 (2000) 3746–3753.
- [63] S. Tsuzuki, K. Honda, T. Uchimaru, M. Mikami, K. Tanabe, *J. Am. Chem. Soc.* 122 (2000) 11450–11458.
- [64] E.D. Glendening, A.E. Reed, J.E. Carpenter, F. Weinhold, *NBO Version 3.1*.
- [65] H.M. Ushay, T.D. Tullius, S.J. Lippard, *Biochemistry* 20 (1981) 3744–3748.
- [66] G.B. Onoa, G. Cervantes, V. Moreno, M.J. Prieto, *Nucleic Acids Res.* 26 (1998) 1473–1480.
- [67] F. Linares, M.A. Galindo, S. Galli, M.A. Romero, J.A.R. Navarro, E. Barea, *Inorg. Chem.* 48 (2009) 7413–7420.
- [68] G. Cervantes, M.J. Prieto, V. Moreno, *Met.-Based Drugs* 4 (1) (1997) 9–18.
- [69] G. Cervantes, S. Marchal, M.J. Prieto, J.M. Perez, V.M. Gonzalez, C. Alonso, V. Moreno, *J. Inorg. Biochem.* 77 (1999) 197–203.
- [70] M.H. Garcia, T.S. Morais, P. Florindo, M.F.M. Piedade, V. Moreno, C. Ciudad, V. Noe, *J. Inorg. Biochem.* 103 (2009) 354–361.
- [71] J. Ruiz, J. Lorenzo, L. Sanglas, N. Cutillas, C. Vicente, M.D. Villa, F.X. Aviles, G. Lopez, V. Moreno, J. Perez, D. Bautista, *Inorg. Chem.* 45 (2006) 6347–6360.
- [72] J. Ruiz, N. Cutillas, C. Vicente, M.D. Villa, G. Lopez, J. Lorenzo, F.X. Aviles, V. Moreno, D. Bautista, *Inorg. Chem.* 44 (2005) 7365–7376.
- [73] G.B. Onoa, V. Moreno, *Int. J. Pharm.* 245 (2002) 55–65.
- [74] J. Ruiz, J. Lorenzo, C. Vicente, G. Lopez, J.M. Lopez-De-Luzuriaga, M. Monge, F.X. Aviles, D. Bautista, V. Moreno, A. Laguna, *Inorg. Chem.* 47 (2008) 6990–7001.
- [75] L.H. Pope, M.C. Davies, C.A. Laughton, C.J. Roberts, S.J.B. Tendler, P.M. Williams, *J. Microsc. -Oxf.* 199 (2000) 68–78.
- [76] M. Yokoyama, A. Satoh, Y. Sakurai, T. Okano, Y. Matsumura, T. Kakizoe, K. Kataoka, *J. Control. Release* 55 (1998) 219–229.
- [77] S.H. Kaufmann, W.C. Earnshaw, *Exp. Cell Res.* 256 (2000) 42–49.
- [78] S.W. Lowe, A.W. Lin, *Carcinogenesis* 21 (2000) 485–495.
- [79] R. Fernández, M. Melchart, A. Habtemariam, S. Parsons, P.J. Sadler, *Chem.-Eur. J.* 10 (2004) 5173–5179.
- [80] T. Hasegawa, T.C. Lau, H. Taube, W.P. Schaefer, *Inorg. Chem.* 30 (1991) 2921–2928.